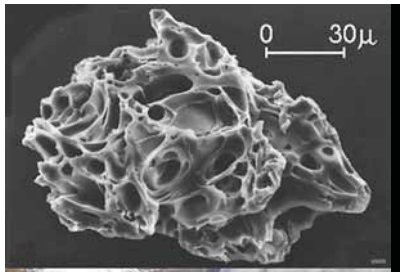

Detection of particle aggregation

Adam Durant
University of Cambridge, UK
NILU, Norway
Michigan Technological University, USA

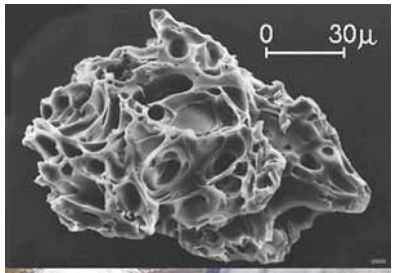

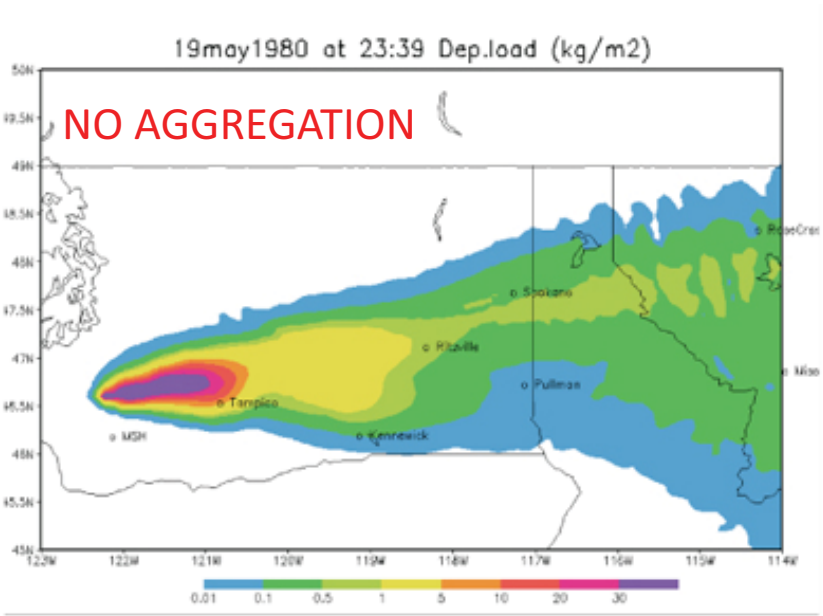

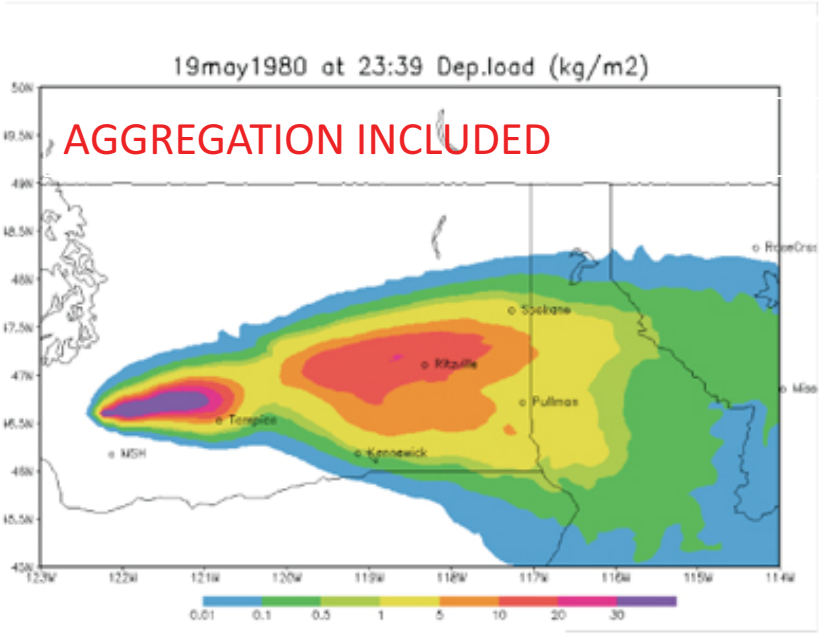

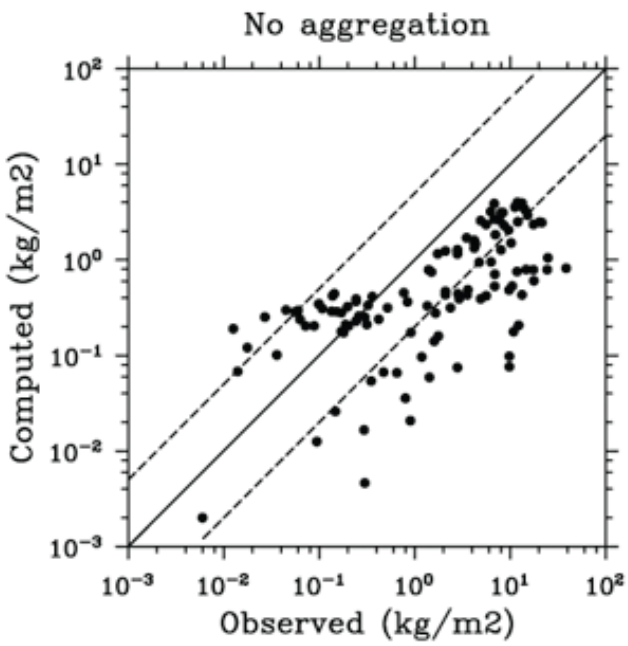

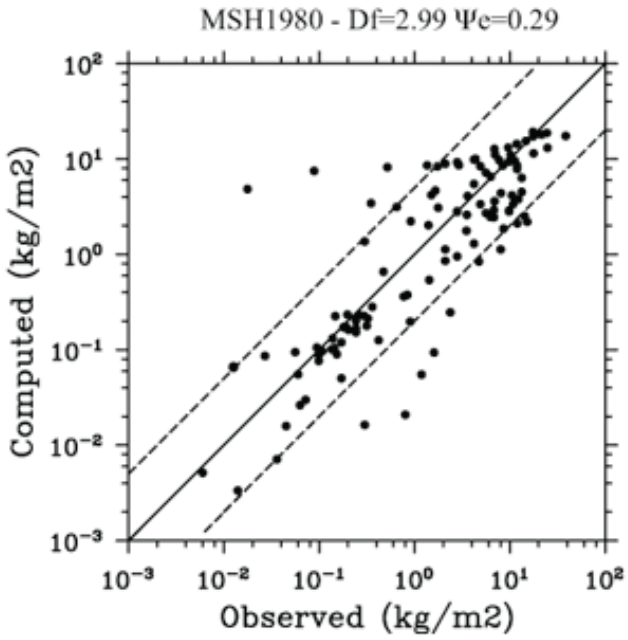

Folch A, Costa A, Durant A, Macedonio G A model for wet aggregation of ash particles in volcanic plumes and clouds: 2. Model application. Journal of Geophysical Research 115(B9):B09202

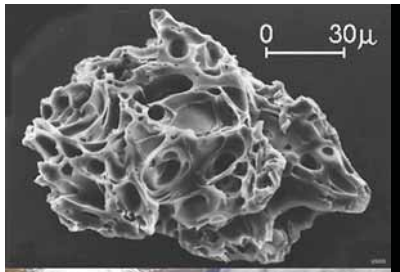

Detection of particle aggregation: Outline

- Visual observation of fallout
- Discrimination in ash deposits
- Conceptual models (hydrometeors)
- Synergies with other techniques
- Data available for aggregation modelling

NILU

UNIVERSITY OF CAMBRIDGE

MichiganTech

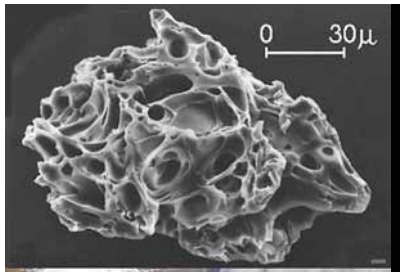

Frozen AL from 23 March 2009 Redoubt eruption (<15 km)

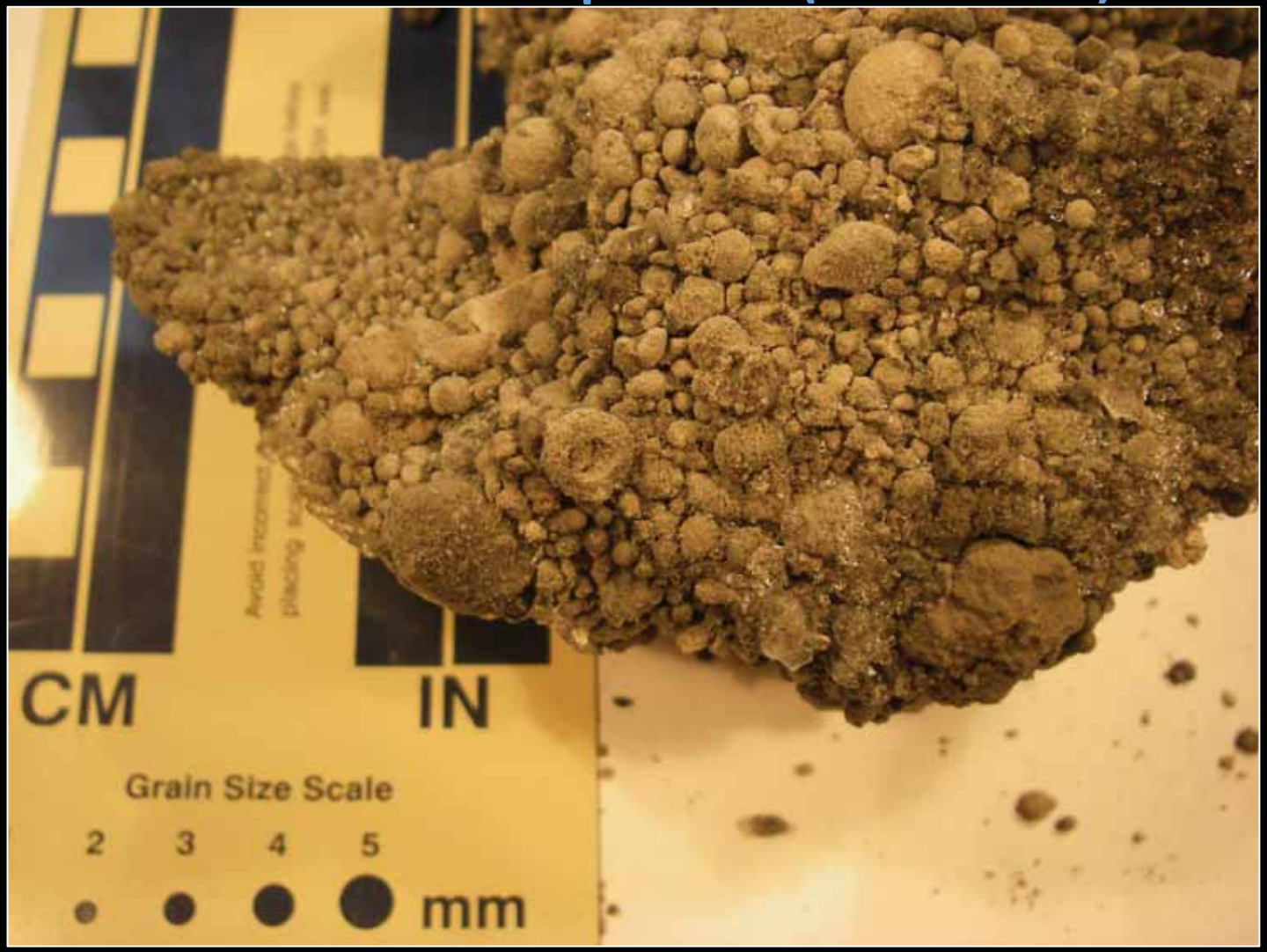

(Image courtesy of K. Wallace, USGS)

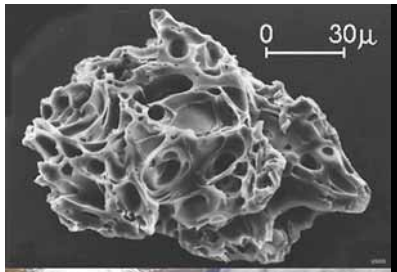

2010 Eyjafjallajökull eruption

5-7 May 2010 (image courtesy Costanza Bonadonna)

NILU

UNIVERSITY OF CAMBRIDGE

MichiganTech

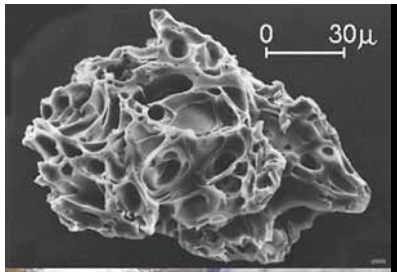

2010 Eyjafjallajökull eruption

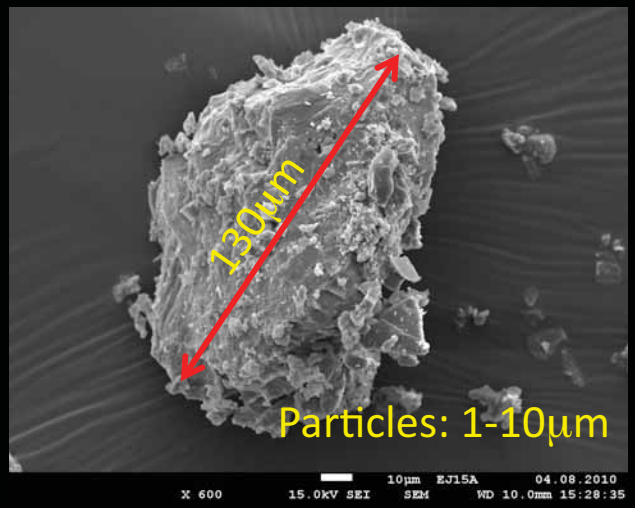

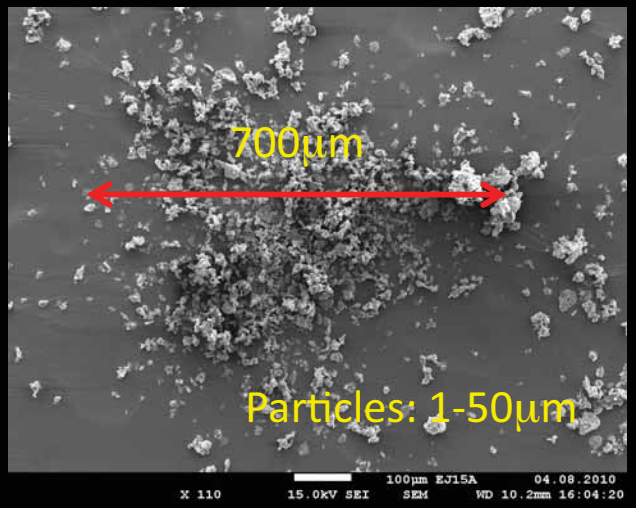

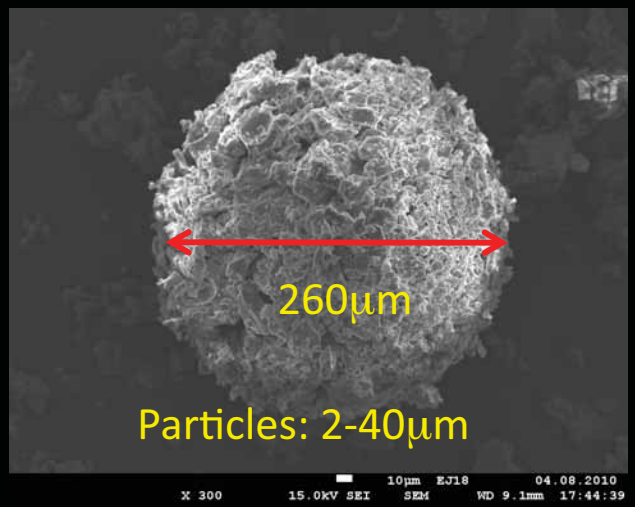

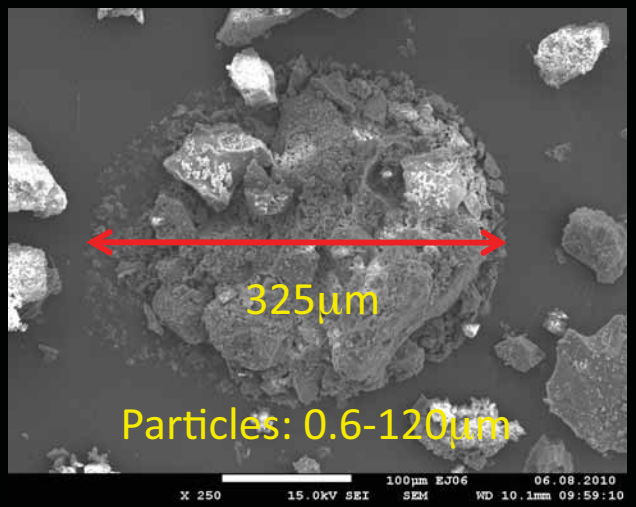

5-7 May 2010 (image courtesy Costanza Bonadonna)

NILU

UNIVERSITY OF CAMBRIDGE

MichiganTech

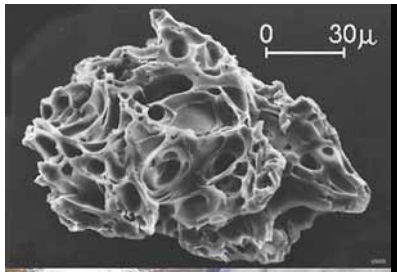

Stratigraphic relationships

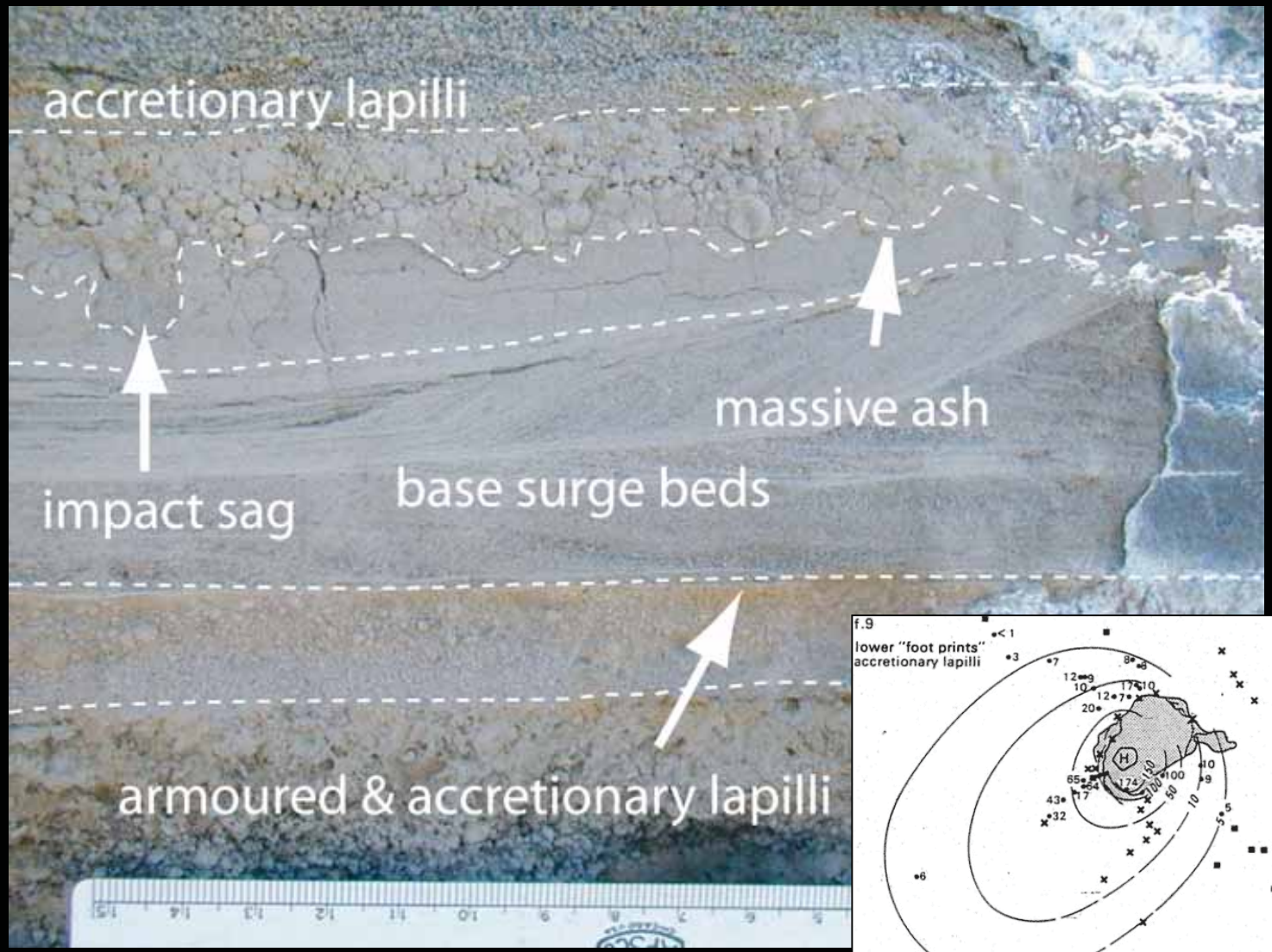

Keanakak'oi Ash, Kilauea, Hawai'i

McPhie et al. 1992

NILU

UNIVERSITY OF CAMBRIDGE

MichiganTech


0 30µ
NILU
UNIVERSITY OF CAMBRIDGE
MichiganTech

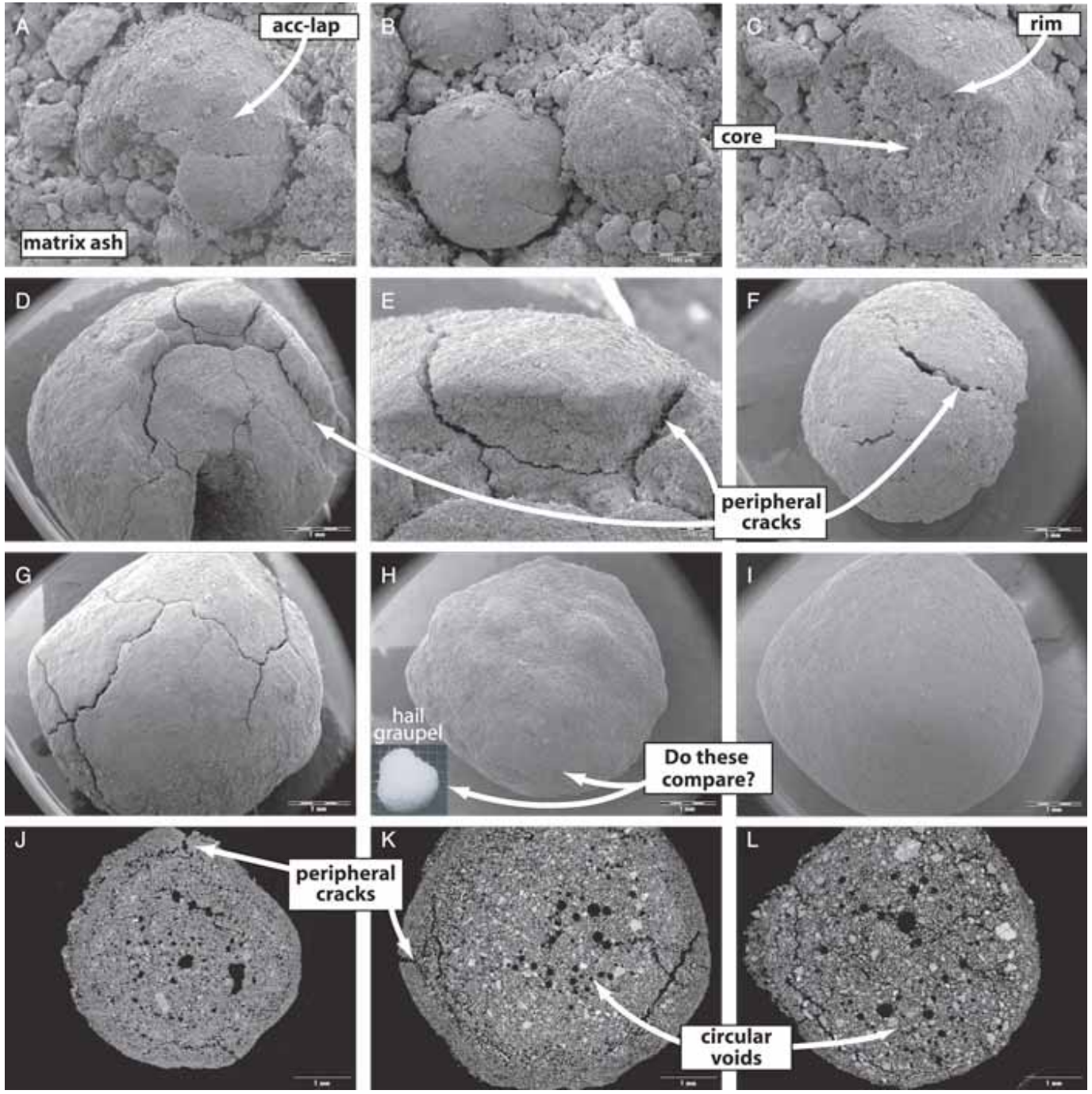
A
acc-lap
matrix ash
B
C
rim
core
D
E
F
peripheral cracks
G
H
hail graupel
Do these compare?
I
J
peripheral cracks
K
circular voids
L

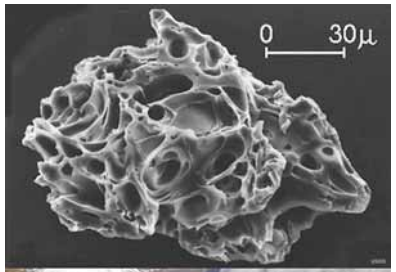

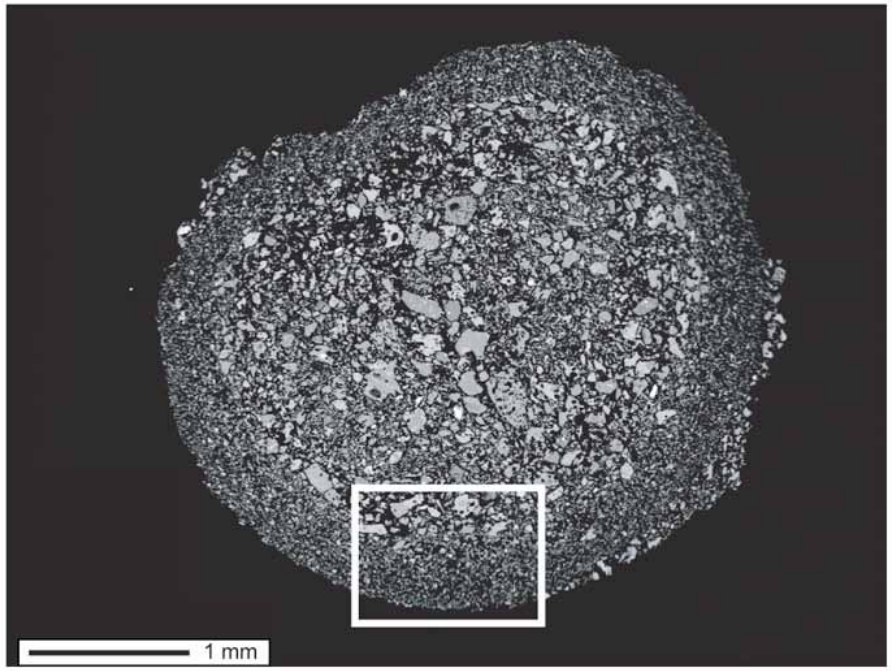

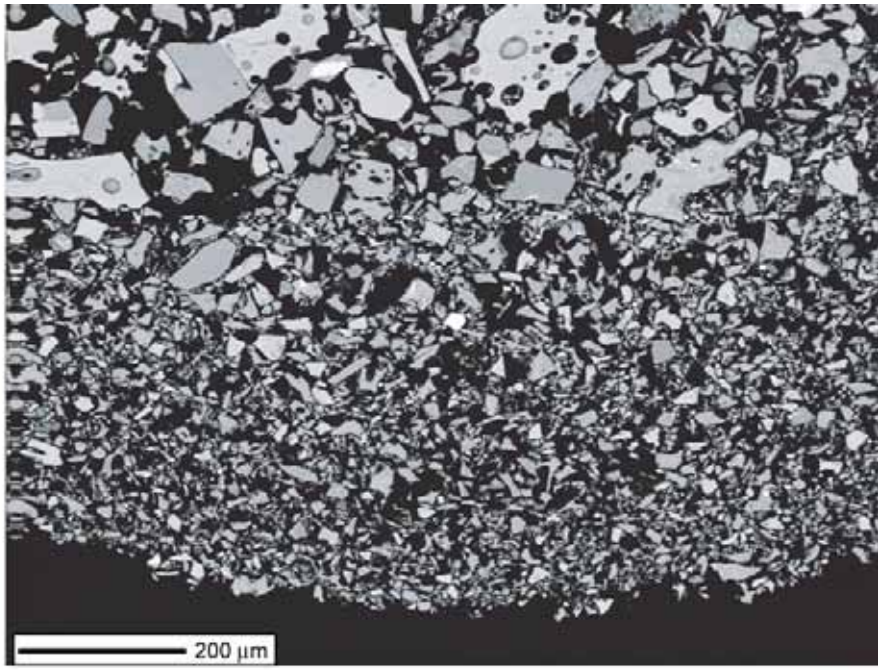

Upper Scoriae 1, Santorini, Greece

Durant and Ernst, in prep

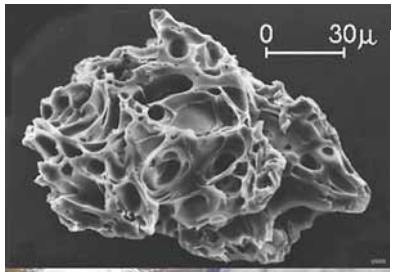

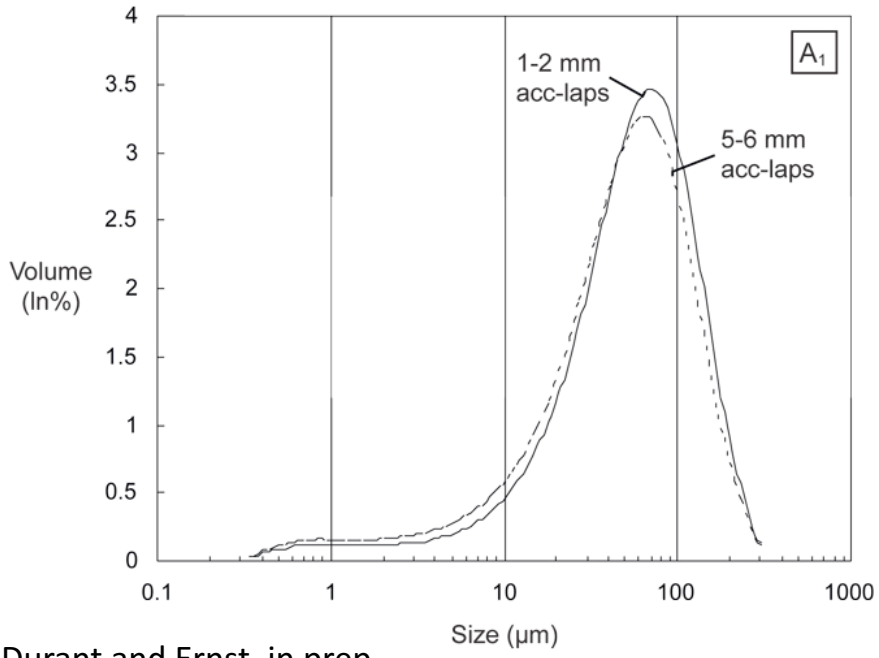

Durant and Ernst, in prep

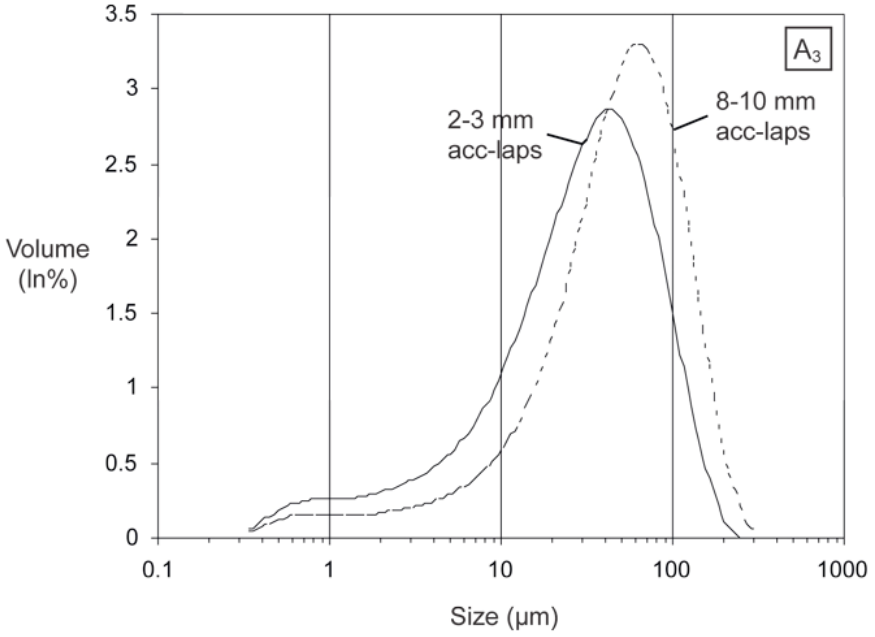

Aggregation coefficient
(liquid water)

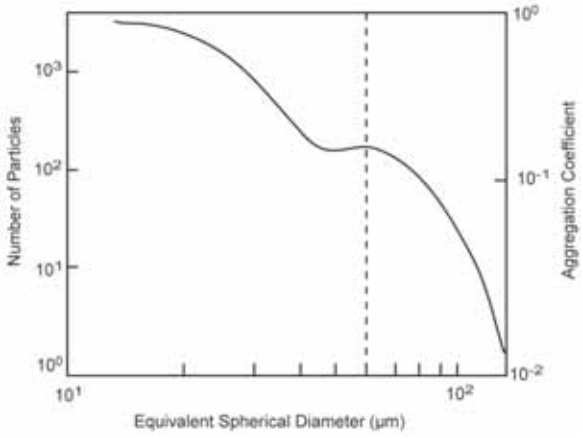

Gilbert and Lane (1994)

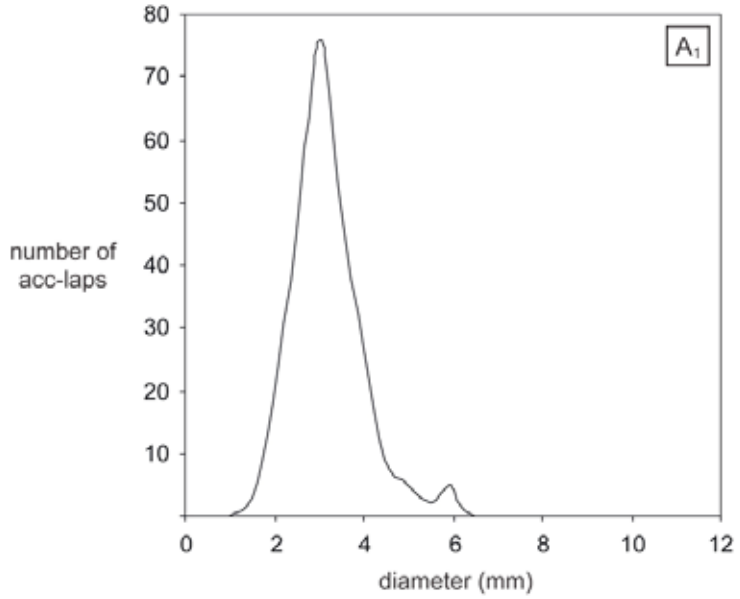

Durant and Ernst, in prep

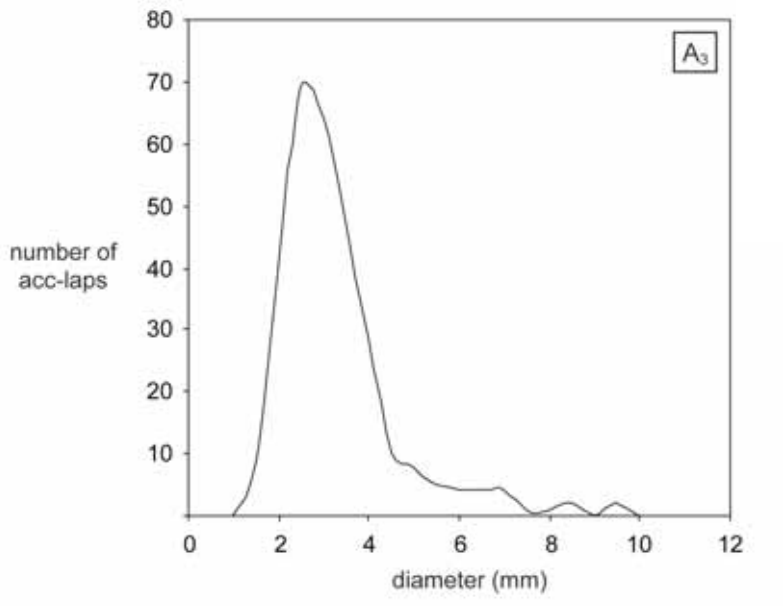

Probability of raindrop break-up

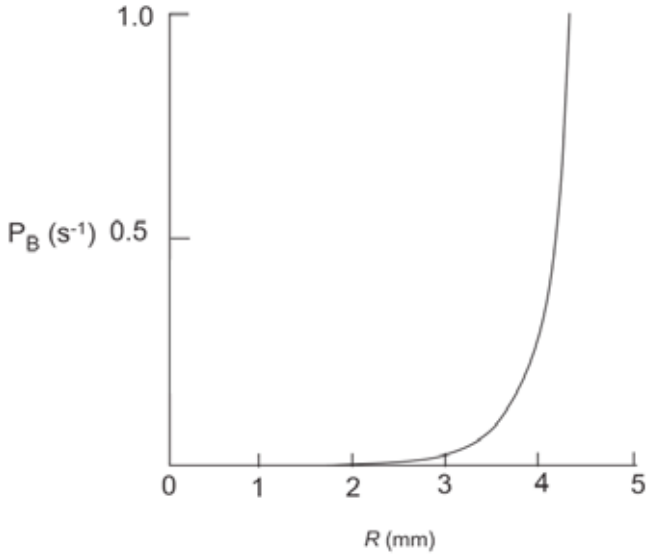

Houze (1993)

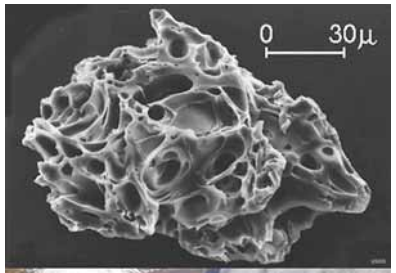

Proximal conceptual model

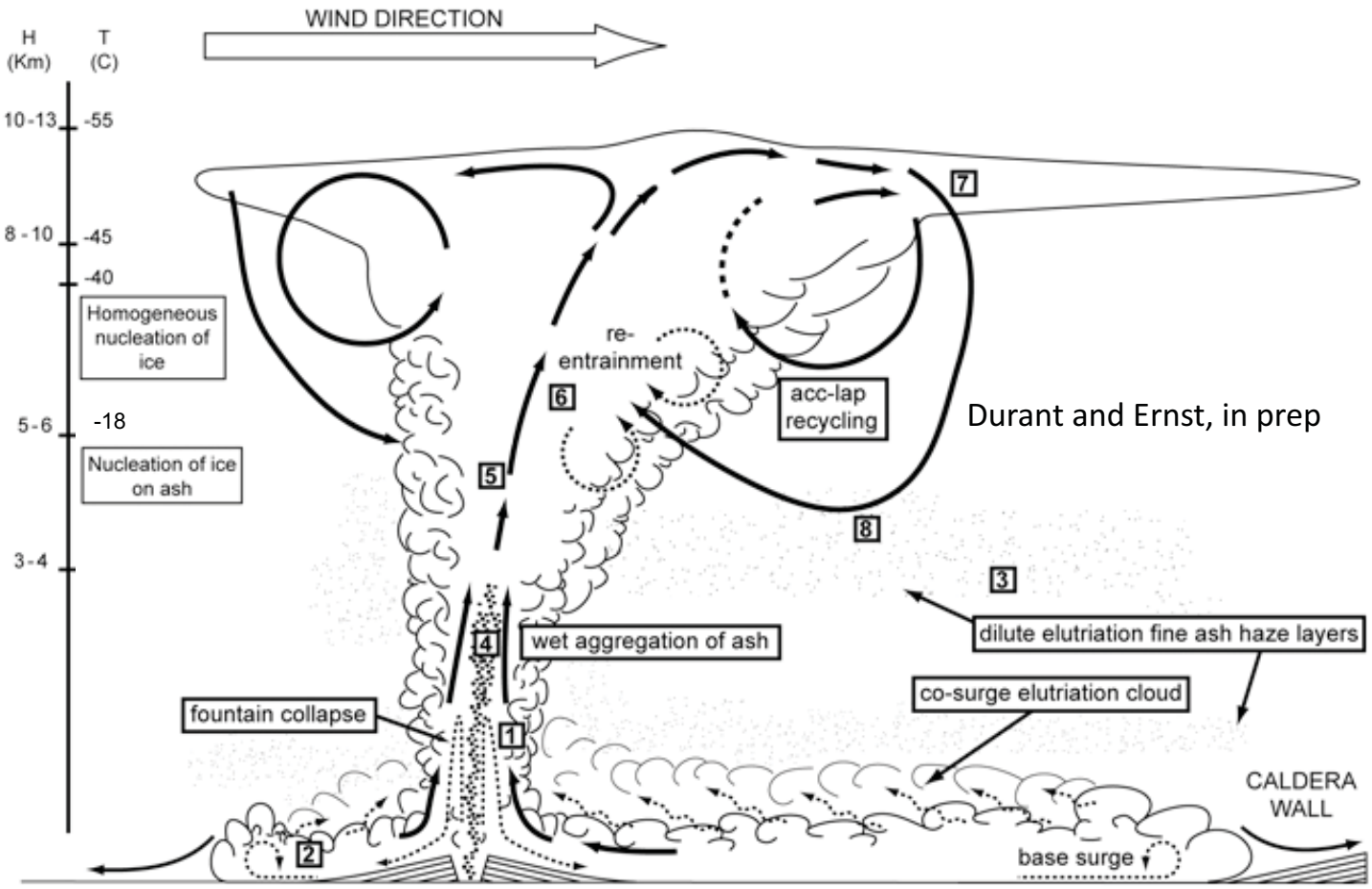

Durant and Ernst, in prep

150-700 km from source

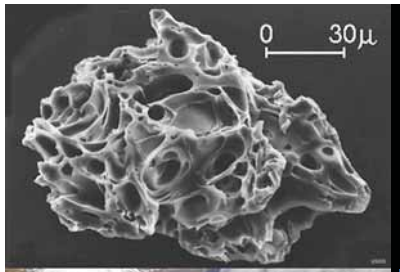

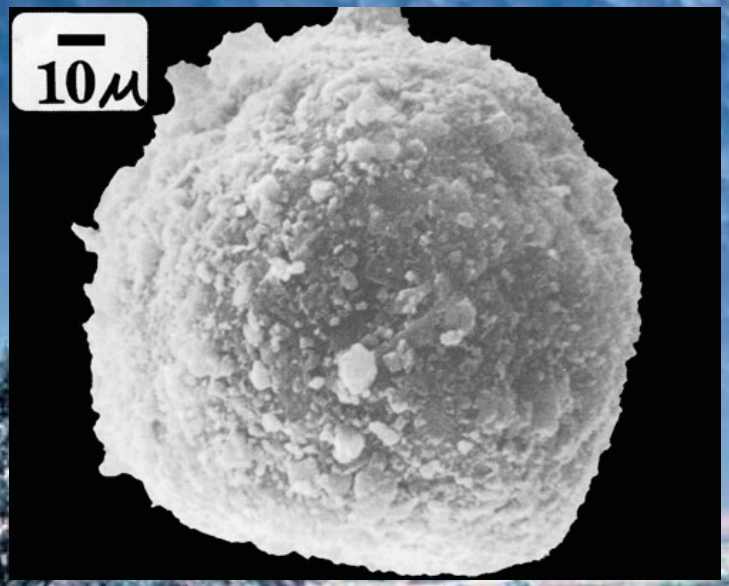

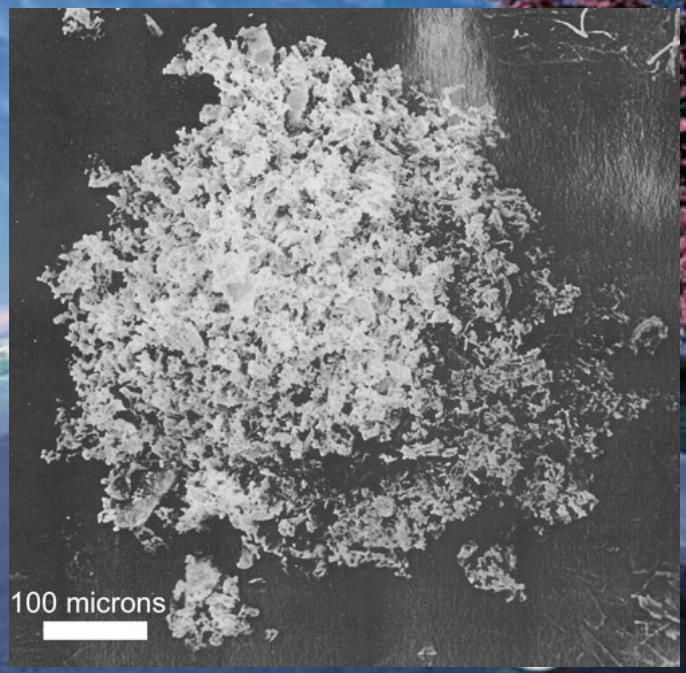

Rose et al. (1981); Sorem (1982); Durant et al. (2009)

NILU

UNIVERSITY OF CAMBRIDGE

MichiganTech

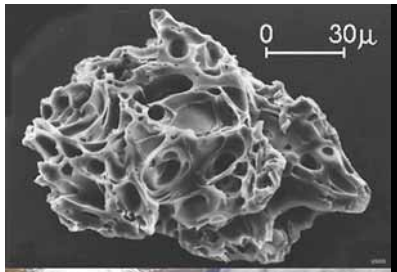

1600 km from source

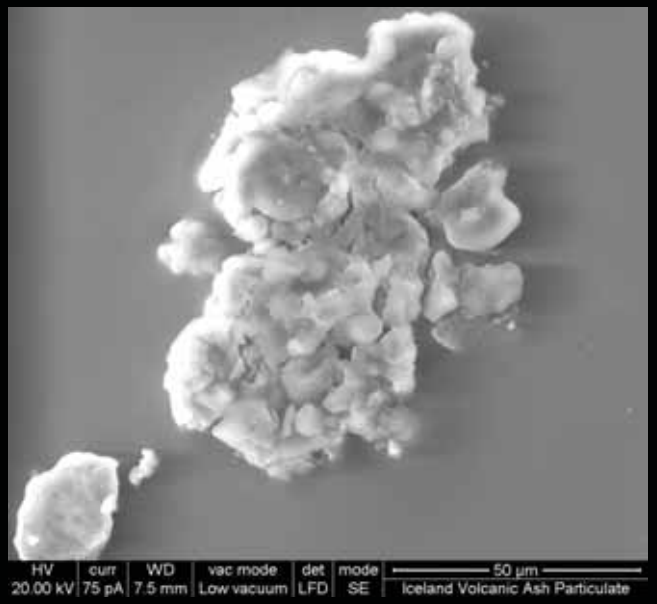

Aggregates from thr Eyjafjallajokul, collected in Loughborough, UK
(image courtesy of Sue Loughlin, BGS)

NILU

UNIVERSITY OF CAMBRIDGE

MichiganTech

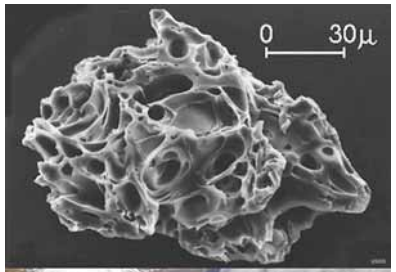

Conceptual model

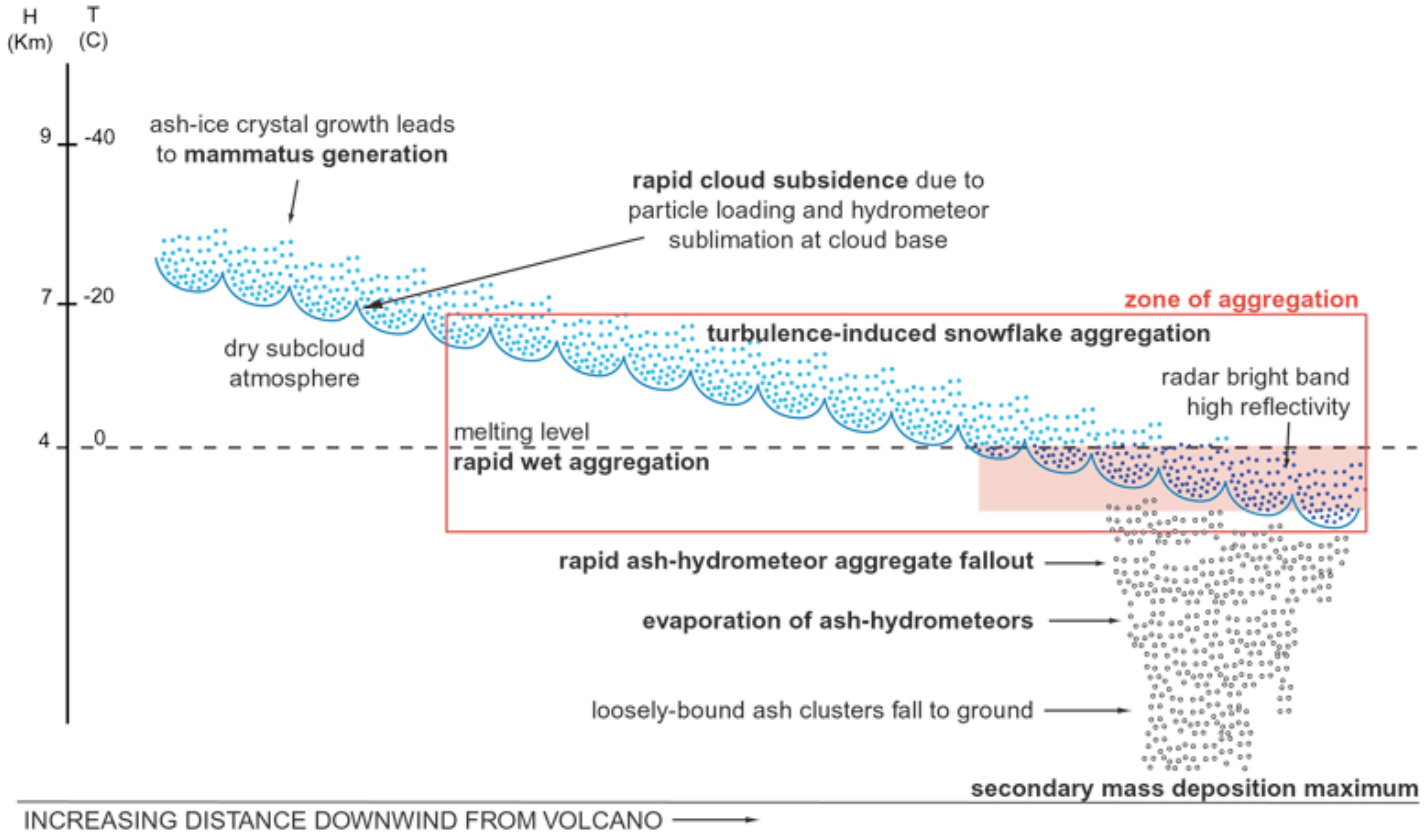

Durant et al. (2009)

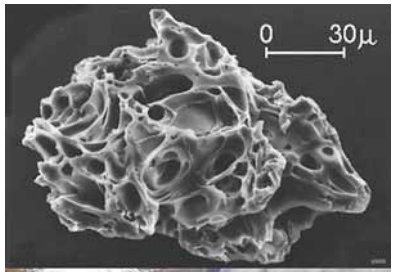

Discrimination in ash deposits

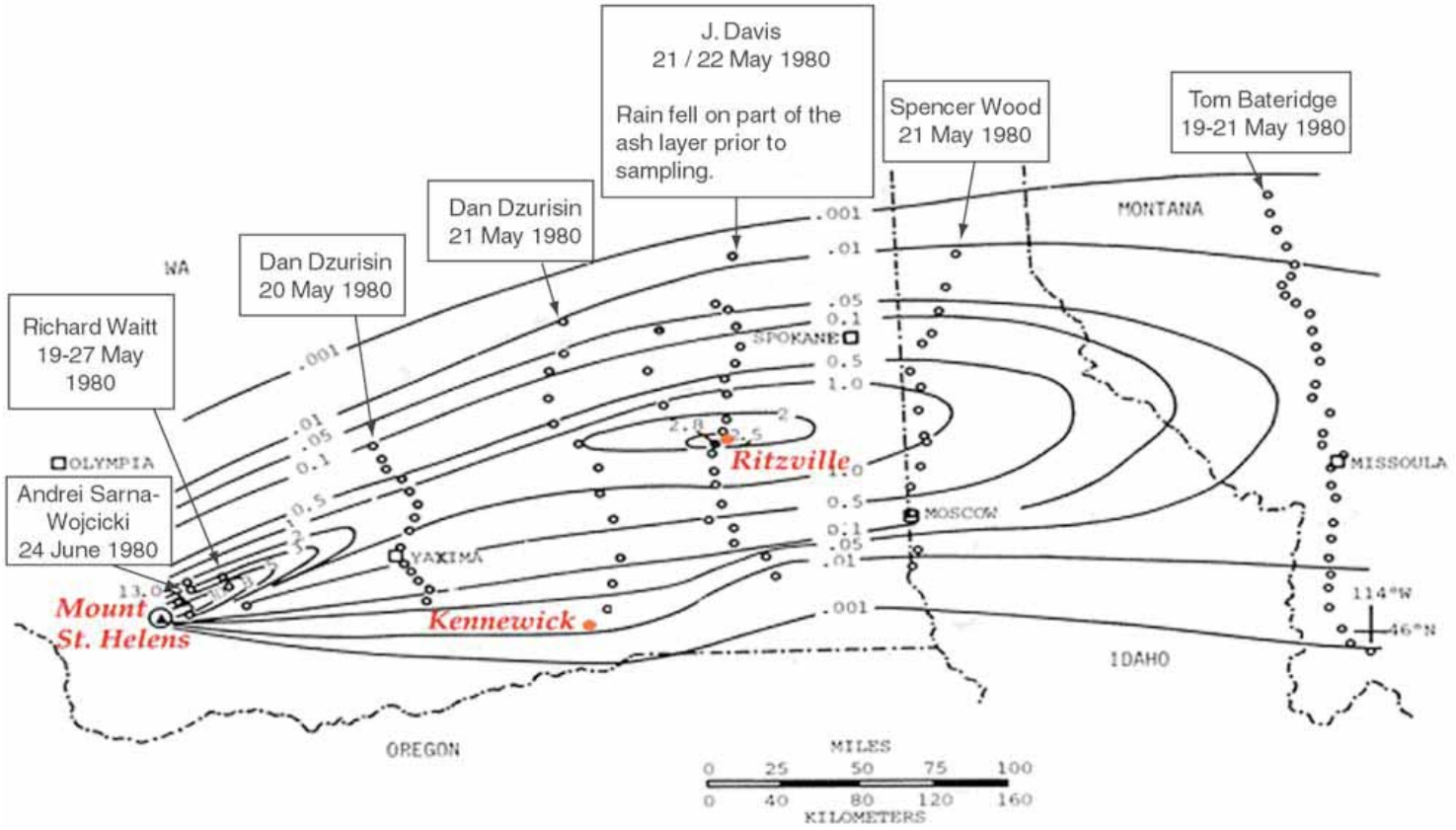

Map adapted from Sarna-Wojcicki et al. (1981), *US Geological Survey Professional Paper, 1250*

Isomass contours in g/cm^3

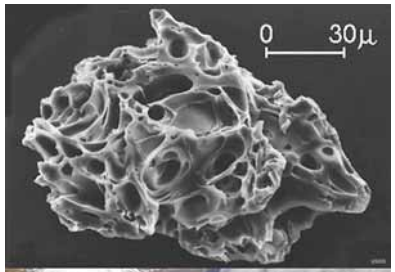

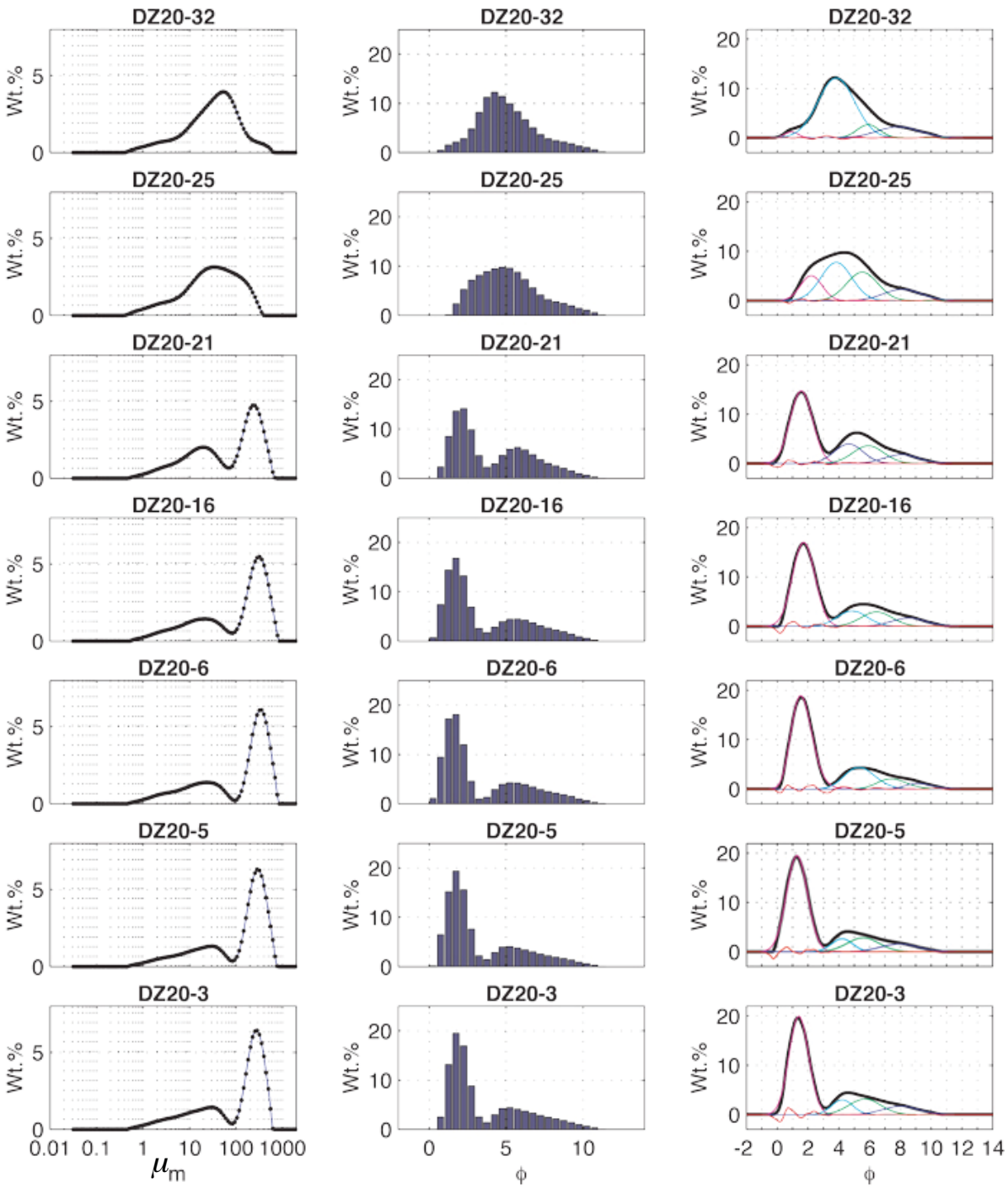

Durant et al. (2009)

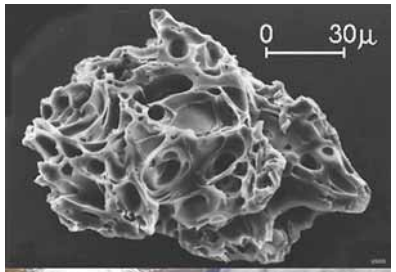

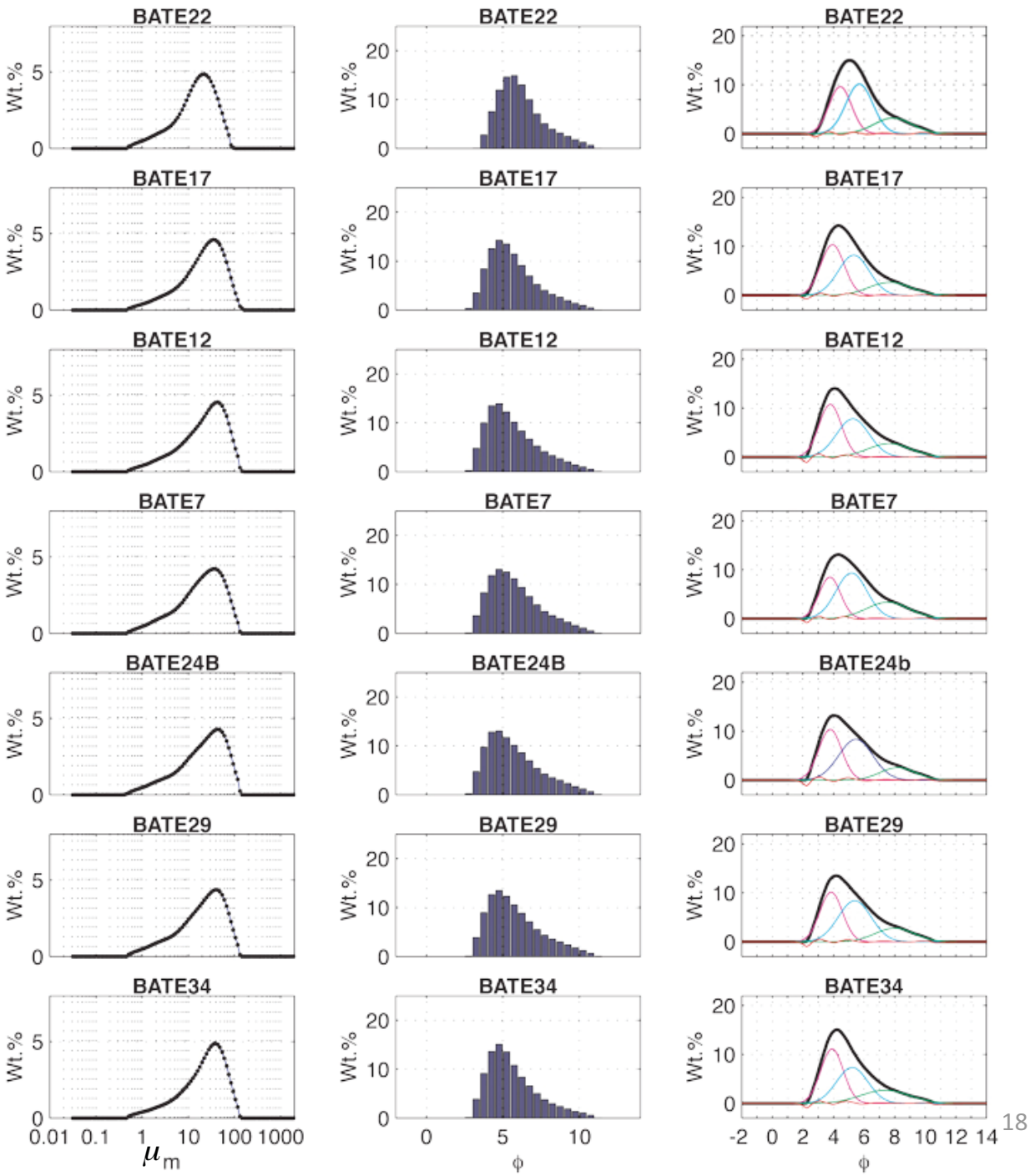

Durant et al. (2009)

Deposit particle size

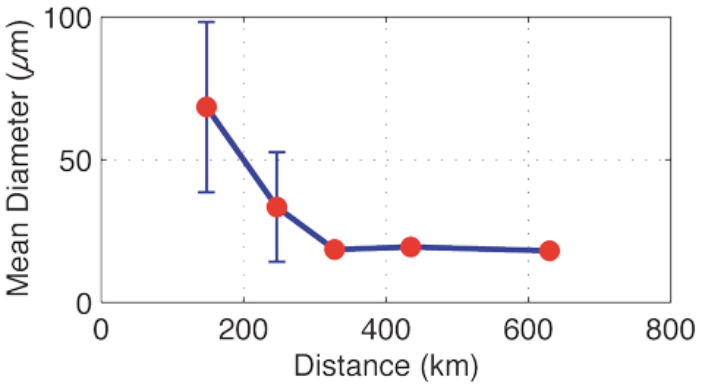

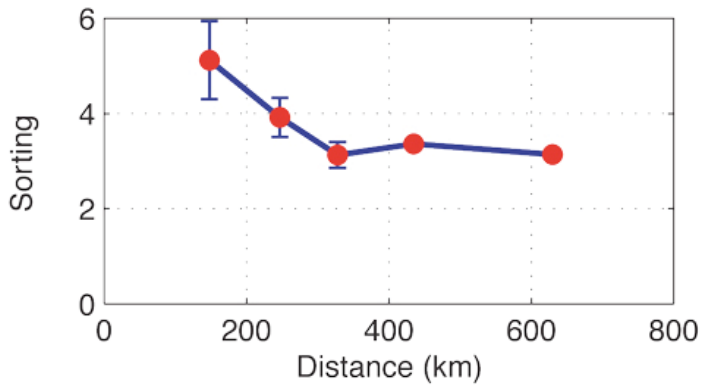

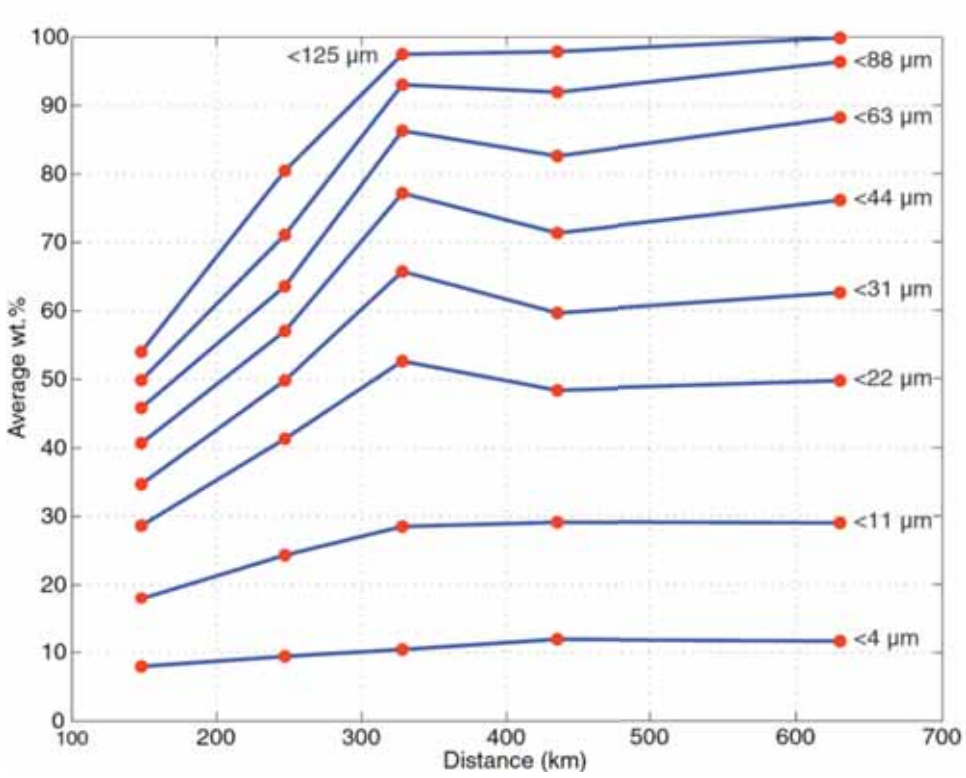

Durant et al. (2009), *J. Geophys. Res.-Solid Earth, 114*

Particle size subpopulations

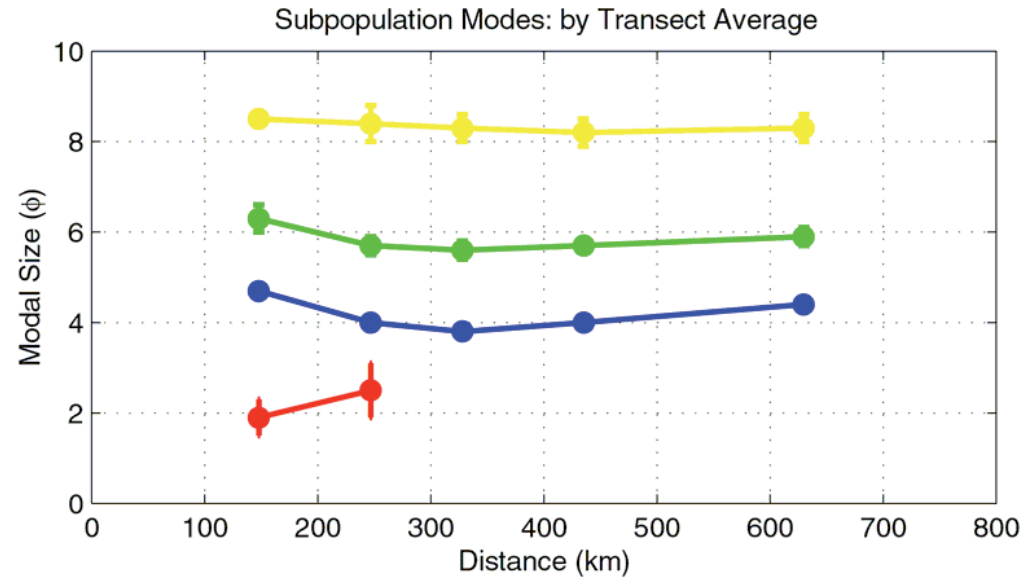

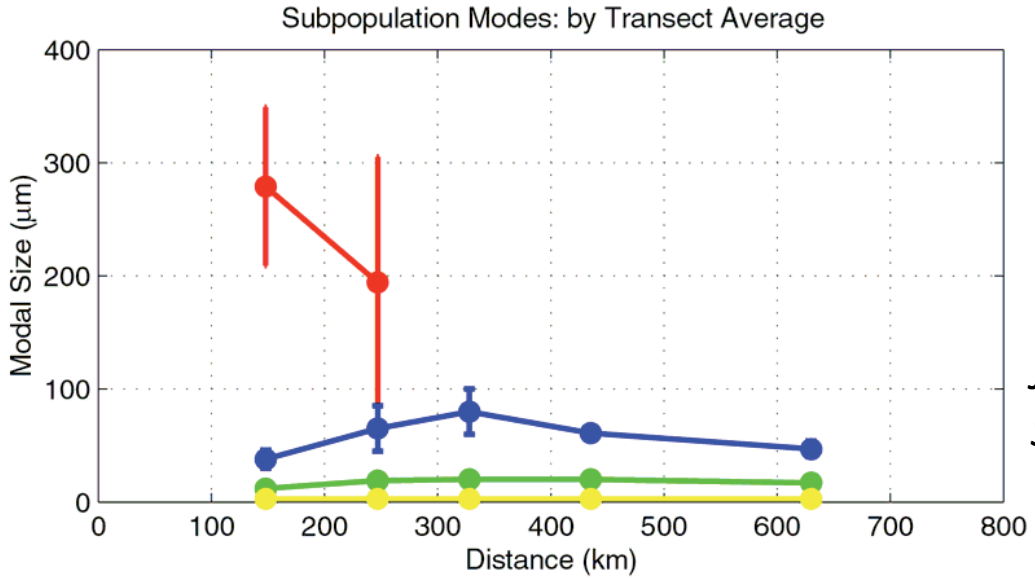

237 µm
58 µm
18 µm
3 µm

Durant et al. (2009), *J. Geophys. Res.-Solid Earth, 114*

Particle size subpopulations

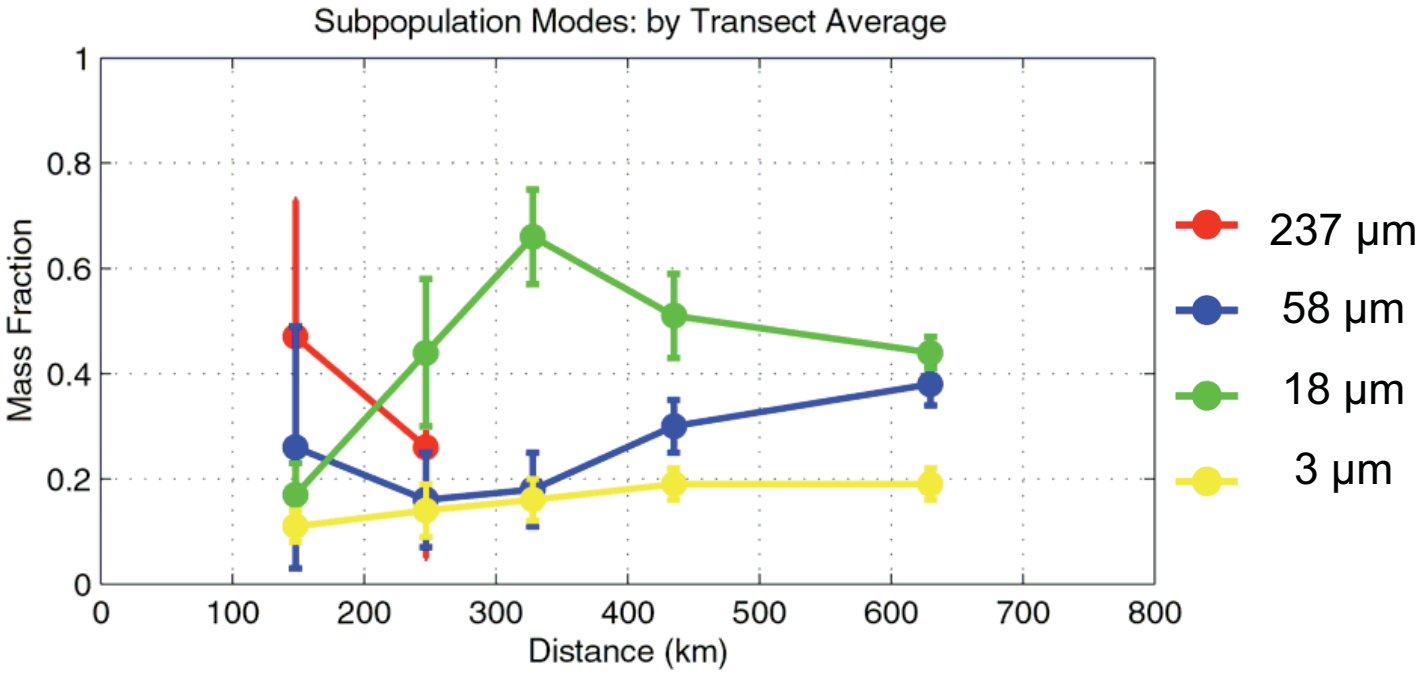

- The proportion of 18 µm subpopulation reaches a maximum at 330 km
- location corresponds to the distal maximum in mass deposition
- location corresponds to observations of mammatus and ash aggregate fall

Durant et al. (2009)

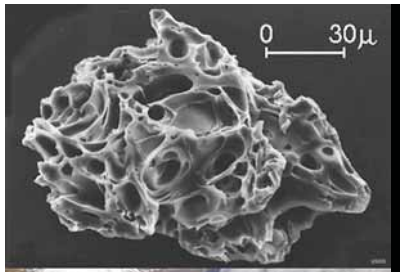

Data available

- Aggregation module inter-comparison
  - MSH80 data
- Distal sedimentation
  - Mount St Helens 18 May 1980
  - 1974 Fuego, Guatemala
  - 1982 El Chichon
  - 1992 Crater Peak eruptions
  - 2008 Chaiten, Chile

NILU

UNIVERSITY OF CAMBRIDGE

MichiganTech

Synergy with other techniques: radar

- Radar reflectivity η :

$$\eta = \sum_i N_i \sigma_i ,$$

where N_i is the number of hydrometeors per unit volume with backscattering cross section σ_i and the summation is over all the hydrometeors in a unit volume

- Radar cross section:

$$\sigma = \frac{\pi^5 |K|^2 D^6}{\lambda^4} ,$$

where λ is the wavelength, *D* the diameter of the hydrometeor, and *K* a dielectric factor related to the refractive index

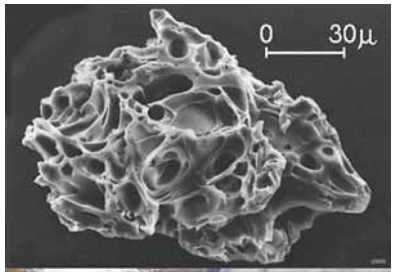

Mount St. Helens 18 May 1980

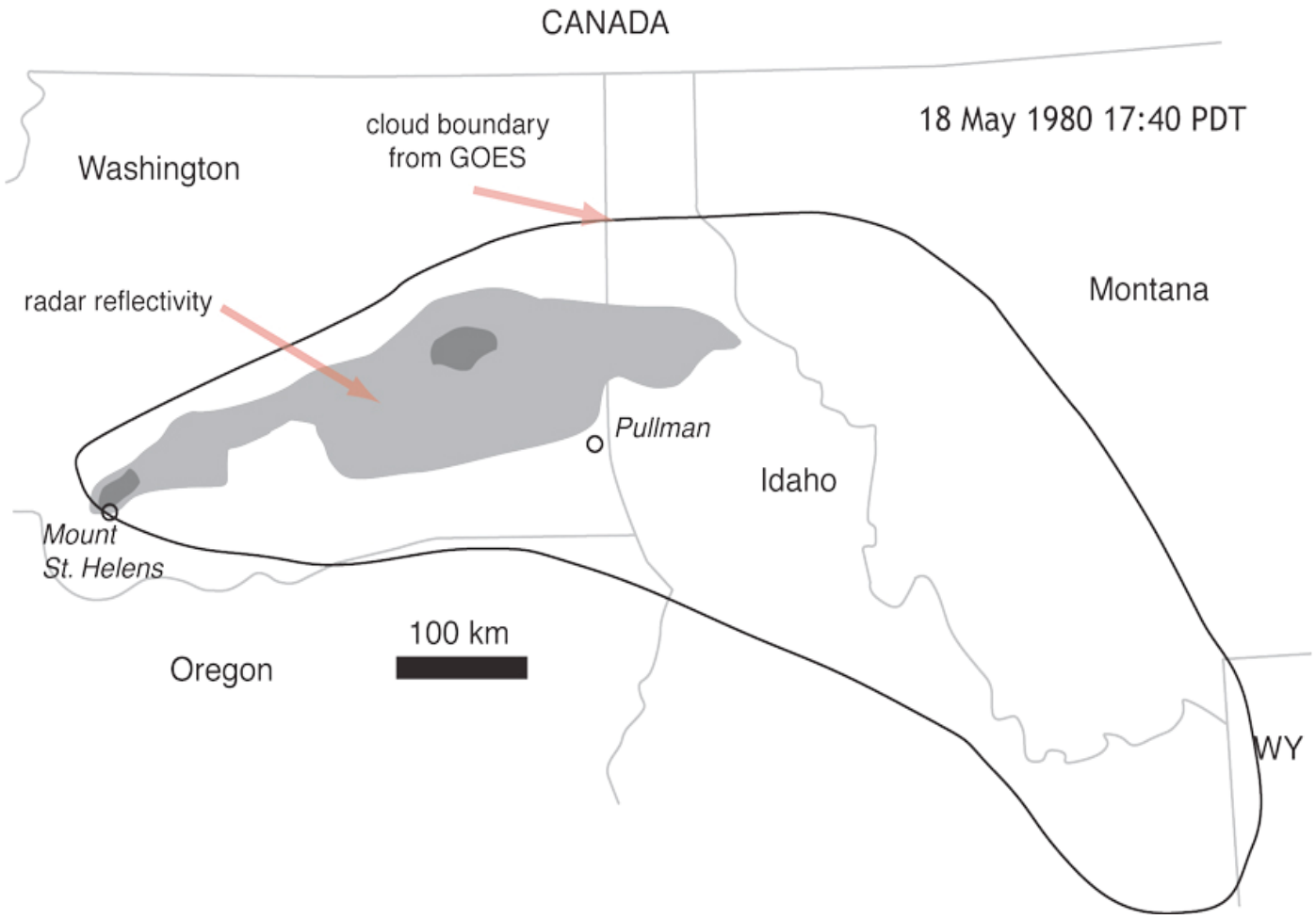

Harris et al. (1981); Durant et al. (2009)

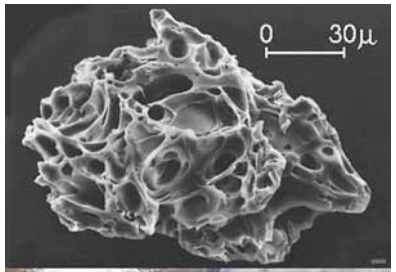

NILU

UNIVERSITY OF CAMBRIDGE

MichiganTech

Radar bright band

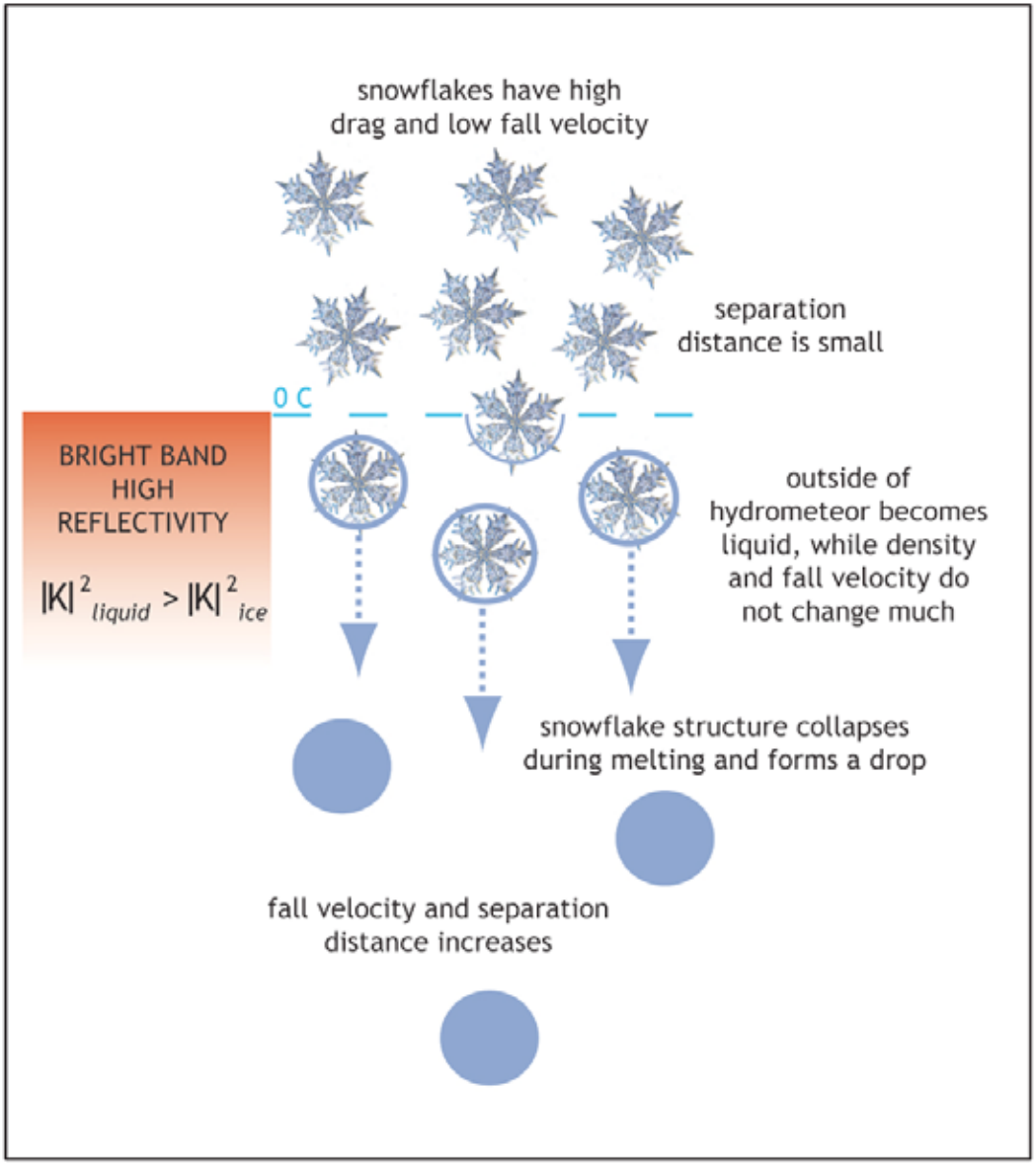

Radar observations: Redoubt 22-23 March 2009

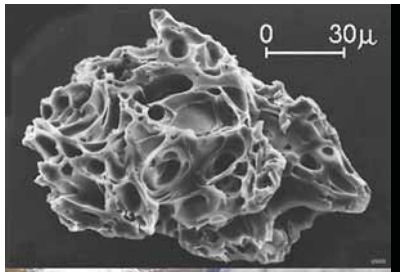

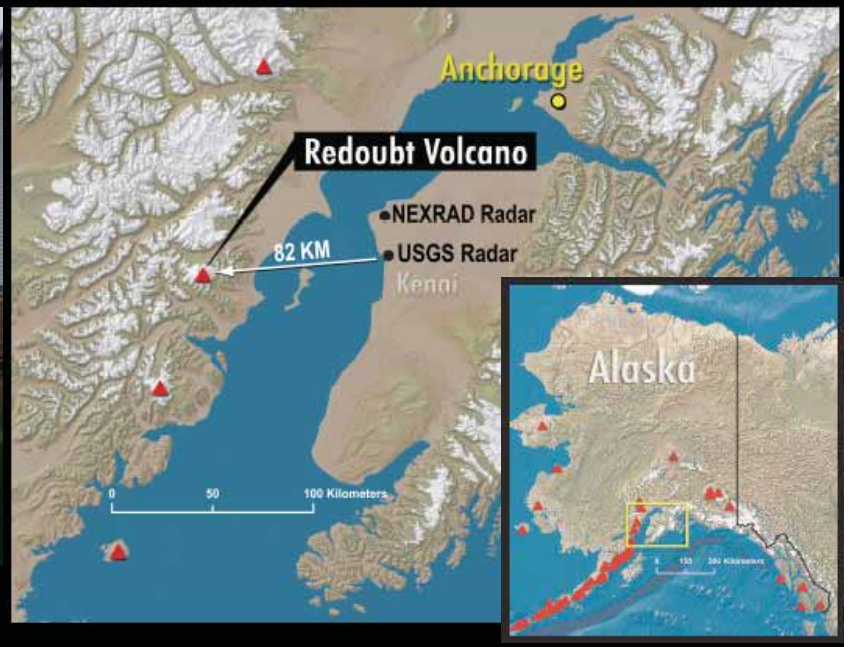

(Courtesy of Dave Schneider, USGS)

NILU

UNIVERSITY OF CAMBRIDGE

MichiganTech

Radial Velocity: 3/23/09 12:45:30 UTC (15 mins)

Altitude: 4.7 km asl; 2.3 km above vent

(Courtesy of Dave Schneider, USGS)

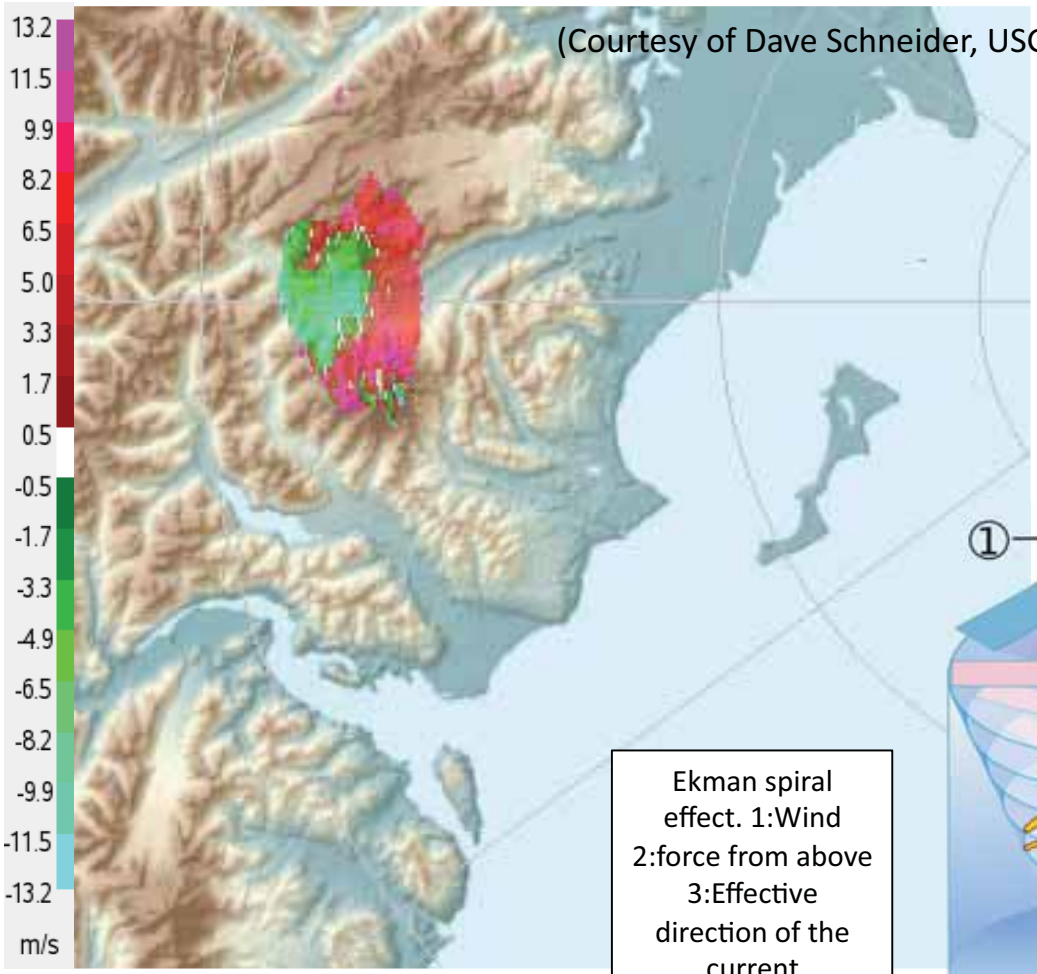

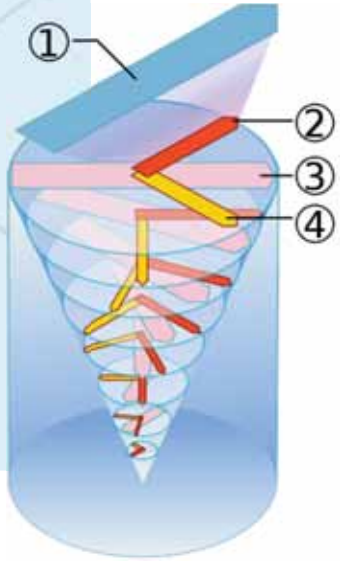

Ekman spiral effect. 1:Wind 2:force from above 3:Effective direction of the current 4: Coriolis effect

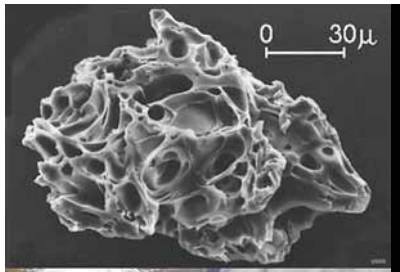

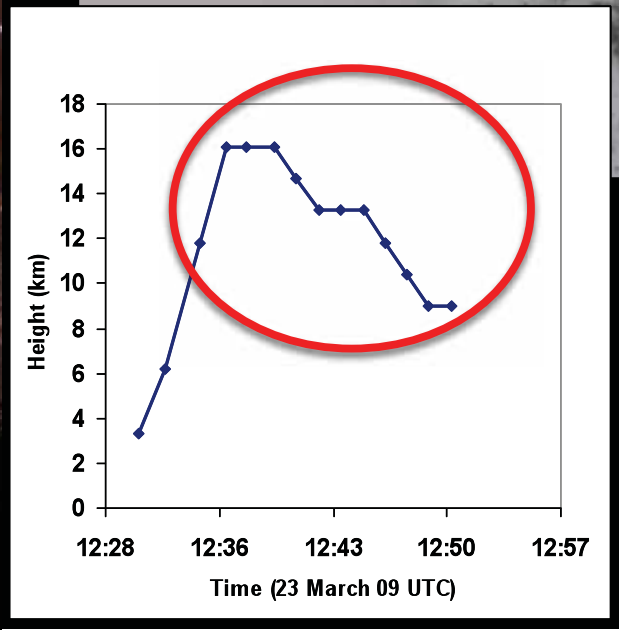

- Plume height decreased by ~7 km in 12 minutes
- Equivalent to a fall rate of ~9 m/s
- Rapid decrease in radar cloud height due to accretionary lapilli formation

(Courtesy of Dave Schneider, USGS)

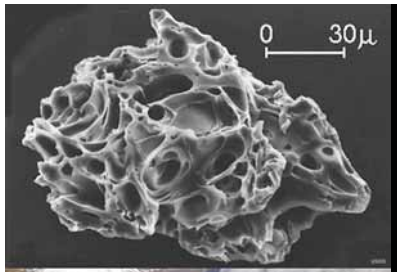

NILU

UNIVERSITY OF CAMBRIDGE

MichiganTech

PLUDIX radar

Doppler Radar (X band - 8 to 12 GHz) to measure vertical velocity and sedimentation rate of falling particles (courtesy of Costanza Bonadonna)

Radar observations of mammatus

RIGHT: Pseudo-RHI plot of (a) reflectivity; and (b) radial velocity for a representative mammatus lobe (from Winstead et al., 2001; Fig. 6), in *Schultz et al.*, [2006].

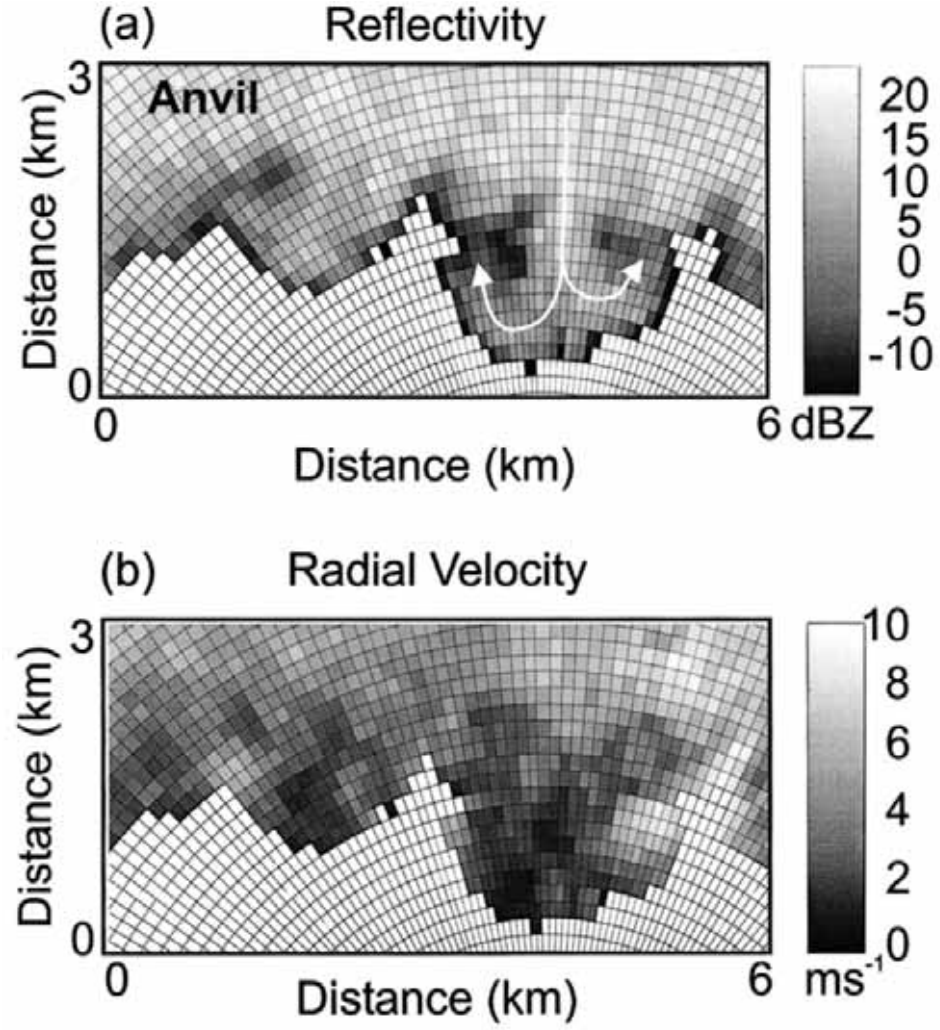

6-km-deep layer of cirrus [*Schultz et al.*, 2006]:

descent of up to 5 ms^{-1} in the mammatus core

weaker ascent up to 1.5 ms^{-1} along the edges

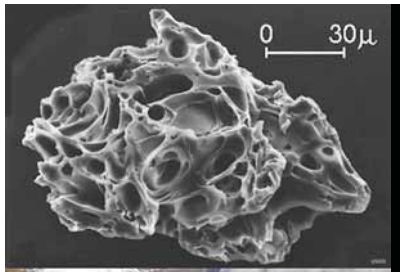

Anatahan IR camera field trials 15-24 June 2003

- Ground-based "clear-sky" and "cloudy-sky" background measurements
- Ship-borne measurements off Anatahan volcano (Pacific Ocean)
- Airborne (horizontal viewing) measurements
- Ground-based measurements on the volcano

Prata AJ, Bernardo C (2009): *Retrieval of volcanic ash particle size, mass and optical depth from a ground-based thermal infrared camera*, **J. Volcanol. Geotherm. Res.**, 186, 91-107

NILU

UNIVERSITY OF CAMBRIDGE

MichiganTech

Ash mass retrieval

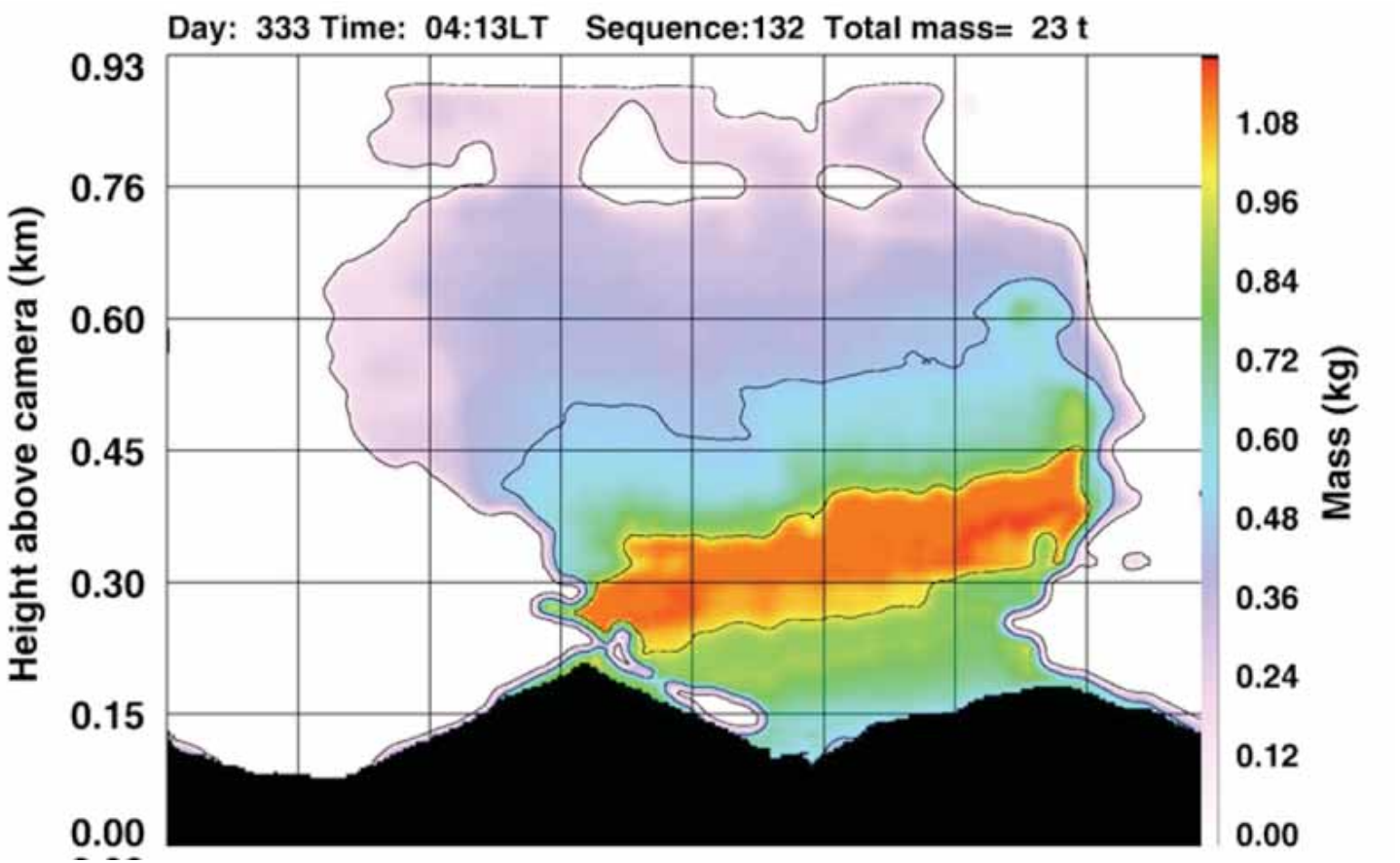

- Function of particle radius (r), infrared optical depth (τ), and zenith viewing angle (θ) for a volcanic cloud with uniform temperature Tc and a background temperature Tb

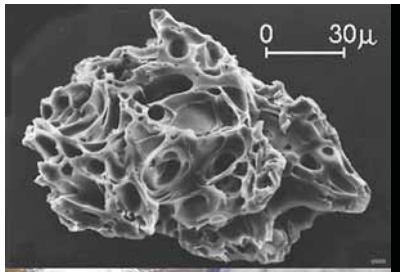

AVOID products

- Discrimination of silicate ash, water droplets, ice clouds, windblown dust, SO_2, water vapour
- Mass loading estimates (gm^{-2}) ahead of aircraft (~ 100 km at 33,000 ft)
- Cloud height estimates

NILU

UNIVERSITY OF CAMBRIDGE

MichiganTech

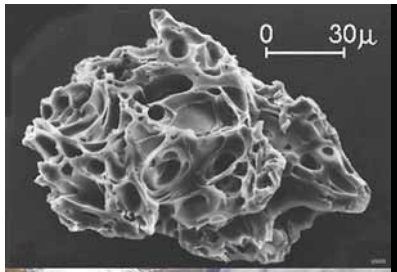

NILU

UNIVERSITY OF CAMBRIDGE

MichiganTech

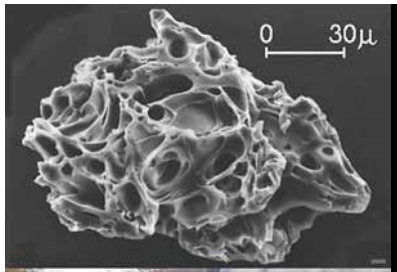

NILU

UNIVERSITY OF CAMBRIDGE

MichiganTech

Courtesy: Ian Davies (**easyJet**)

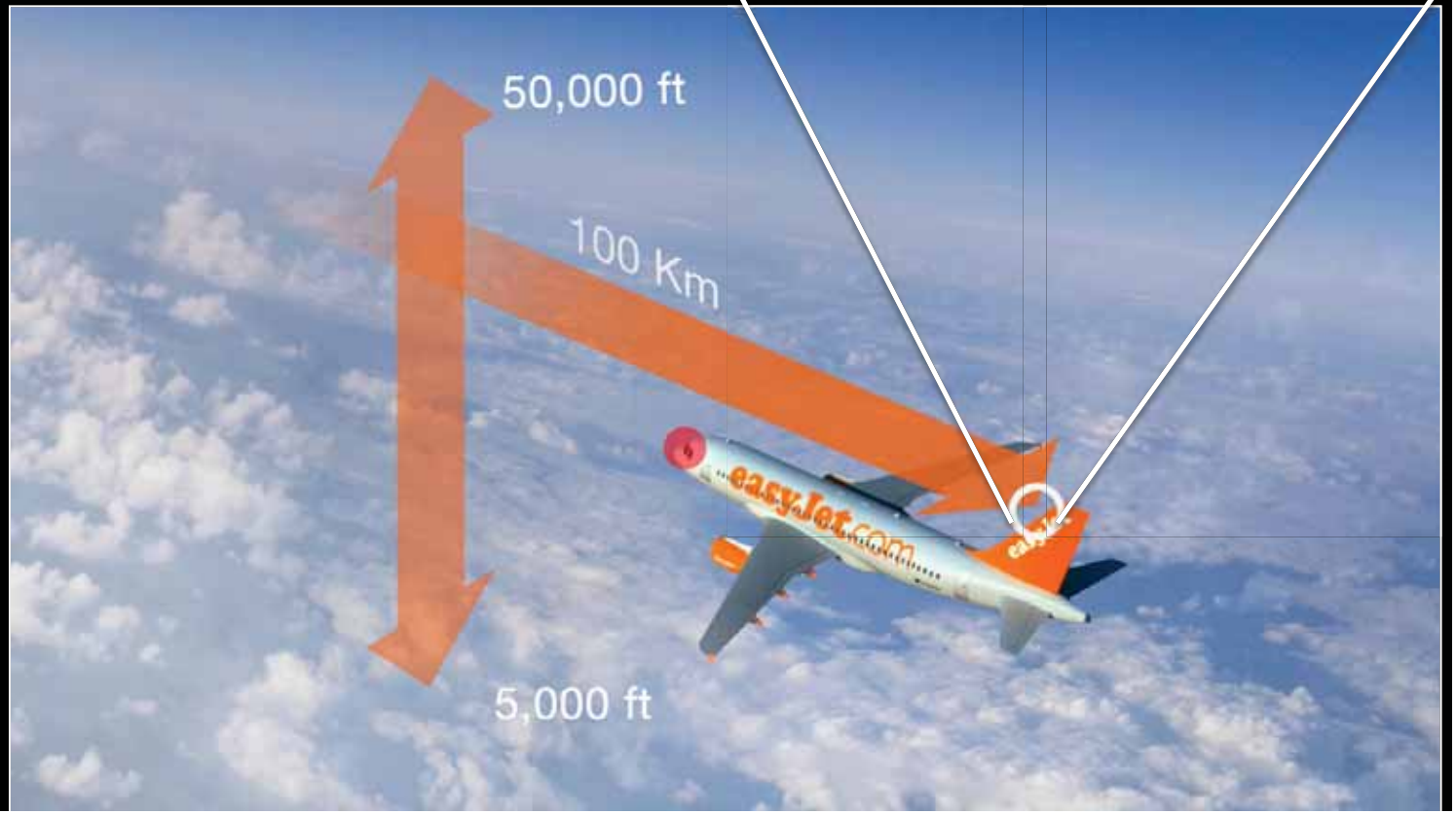

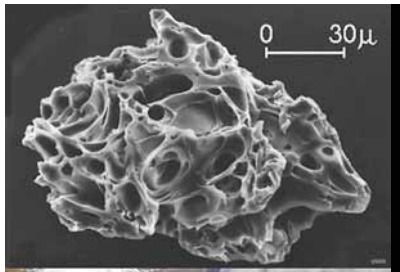

Simulated ash cloud navigation using **AVOID**

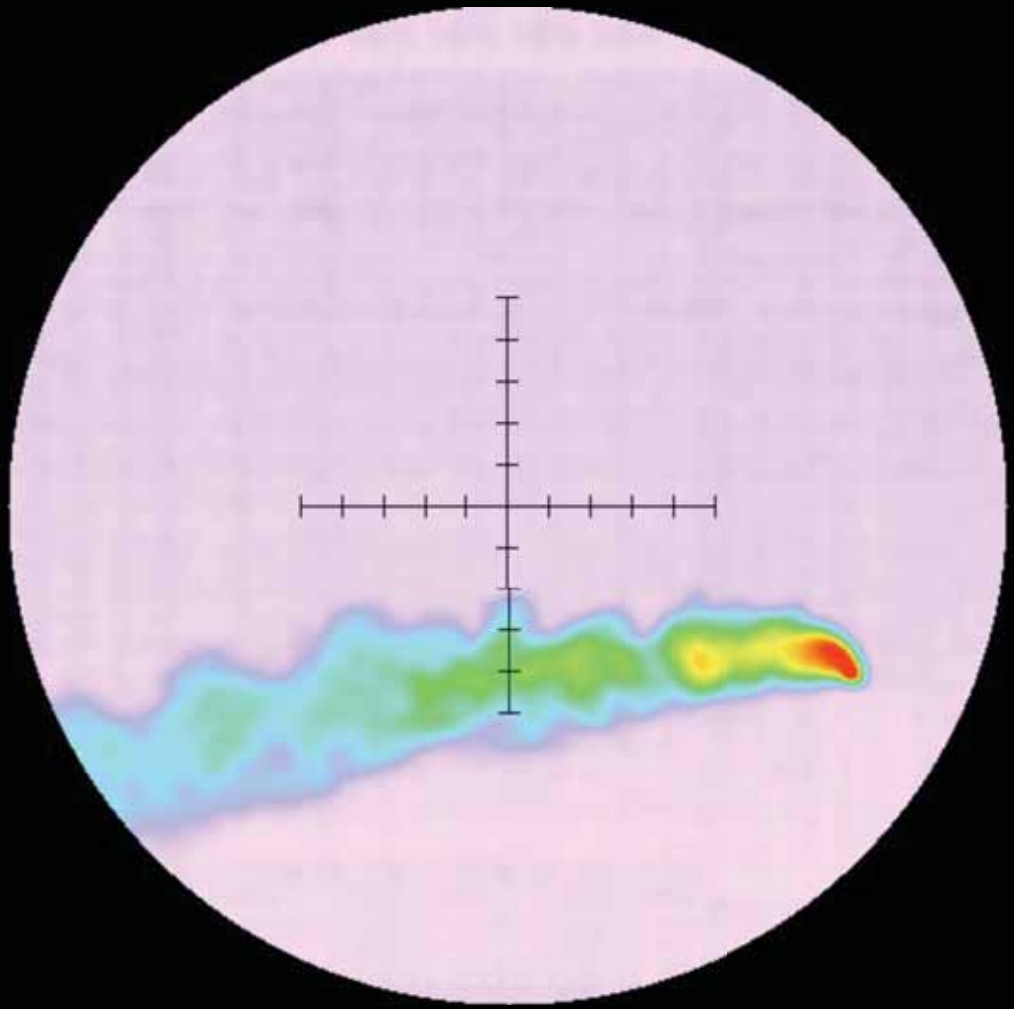

NILU

UNIVERSITY OF CAMBRIDGE

MichiganTech

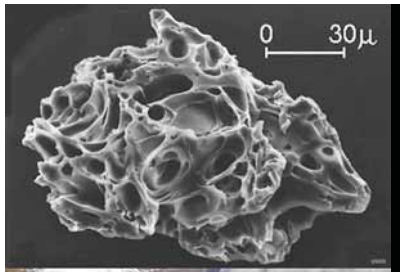

Integrated measurement strategy

- Airborne particle number distributions and particle size
  - In situ measurements (number conc)
  - Remote sensing (sun photometer, lidar)
- Liquid water content
  - In situ (radiosonde)
  - Remote sensing (radar, lidar)
- Ice water content
  - In situ (radiosonde)
  - Remote sensing (lidar, satellite TIR)
- Electric charge measurements
  - Lightening strikes, potential difference

NILU

UNIVERSITY OF CAMBRIDGE

MichiganTech